John von Neumann Institute for Computing

Dynamic Properties via Fixed Centroid Path Integrals

Rafael Ramírez, Telesforo López-Ciudad

published in

Quantum Simulations of Complex Many-Body Systems: From Theory to Algorithms, Lecture Notes,
J. Grotendorst, D. Marx, A. Muramatsu (Eds.),
John von Neumann Institute for Computing, Jülich,
NIC Series, Vol. **10**, ISBN 3-00-009057-6, pp. 325-360, 2002.

http://www.fz-juelich.de/nic-series/volume10

Dynamic Properties via Fixed Centroid Path Integrals

Rafael Ramírez and Telesforo López-Ciudad

Instituto de Ciencia de Materiales
Consejo Superior de Investigaciones Científicas (C.S.I.C.)
Cantoblanco, 28049 Madrid, Spain
E-mail: {*ramirez, tito.lopez*}*@icmm.csic.es*

Computer simulations of complex many-body systems by Centroid Molecular Dynamics (CMD) are a practical route for the calculation of time dependent properties, i.e., time correlation functions, of quantum systems in thermodynamic equilibrium. The CMD approach can be readily implemented into standard codes for Monte Carlo or molecular dynamics path integral simulations of static properties. However, the advantageous property of being readily implementable is not a prerequisite for the even more important property of predicting correct results. In this context, the rigorous formulation of CMD is an important goal to understand its capability to describe real time quantum dynamics. Our purpose in this contribution is fourfold: (i) to present a derivation of CMD and a related dynamic approach within the Schrödinger formulation, as an alternative to the usual route based on the path integral formulation; (ii) to analyze the capability of these approaches in the study of simple exact solvable models; (iii) to review the CMD applications done on a variety of systems and properties; (iv) to summarize the most important open problems for CMD applications.

1 Introduction

The formulation of statistical mechanics using path integrals (PI) provides a practical computational route for the simulation of *static properties* of quantum many-body systems in thermodynamic equilibrium.[1–5] One of the most suggestive pictures derived from the PI approach is the so-called *quantum-classical isomorphism*. This isomorphism states that the statistical behavior of a set of quantum particles can be mapped onto a classical model of interacting "ring polymers". In more precise terms, the canonical partition function, Z, of N quantum particles results to be identical to the *classical* partition function of N interacting "ring polymers",

$$Z \equiv Z^{cla}_{ring-polymers} \ . \tag{1}$$

The isomorphism opens the possibility to extend classical simulation methods such as Monte Carlo (MC) and molecular dynamics (MD) to the quantum domain. Thus, static properties of quantum systems, i.e., those that can be derived from the partition function Z, can be readily computed by classical simulations of ring polymers.

A second version of the quantum-classical isomorphism was worked out by Feynman and Hibbs in 1965.[1] These authors realized that the classical partition function of the N rings polymers can be alternatively rewritten in terms of the N *centroid positions* or center of masses of the ring polymers. As a result, Feynman and Hibbs defined an *effective classical potential*, V_{ecp}, that allowed them to formulate a new isomorphism: The partition function of the N quantum particles, Z, turns out to be identical to the *classical* partition function of N particles moving in the effective classical potential, V_{ecp},

$$Z \equiv Z^{cla}_{ecp} \ . \tag{2}$$

The computation of V_{ecp} is a difficult task that implies solving *fixed centroid path integrals*, that are defined as standard path integrals with a geometrical constraint that fixes the centroid position. There exists an important body of literature on methods based on the effective classical potential and fixed centroid path integrals. Many interesting works focus on the formulation of variational approximations for V_{ecp}, that can be applied to compute static properties.[1,6–9] Other relevant application is the formulation of the PI quantum transition state theory (QTST), a kinetic approach to compute rate constants of thermally activated quantum processes.[4,10–15]

Based on the success of the quantum-classical isomorphism for the simulation of static properties, one may wonder if there exists some kind of *dynamic* quantum-classical isomorphism, that would allow us to derive *exact* quantum dynamics from *classical dynamics* of either the "ring polymers" or their centroids. Unfortunately, the answer is not. The reason is that dynamic properties, like time correlation functions, can not be derived from the knowledge of the partition function. Thus, an identity in the partition functions of the quantum system and its classical isomorph, does not imply a coincidence in the corresponding dynamic properties. However, the suggestive picture provided by the quantum-classical isomorphism has motivated the sought of an *approximate* description of real time quantum dynamics in terms of classical dynamics of the corresponding classical isomorph.

The most practical approximation developed so far is centroid molecular dynamics (CMD), formulated by Cao and Voth in 1994.[16–20] CMD solves the dynamic equations of classical particles moving in the effective classical potential, V_{ecp}. For the simple case of a particle of mass m, whose centroid position and momentum are (X, P), the CMD equations read

$$\dot{X} = \frac{P}{m} \, , \tag{3}$$

$$\dot{P} = f_m \, . \tag{4}$$

where the dot indicates a time derivative, and f_m is the *mean force*, defined as the position derivative of the effective classical potential

$$f_m = -\frac{dV_{ecp}}{dX} \, . \tag{5}$$

The capability of CMD to describe real time quantum dynamics lies on the *assumption* that the effective classical potential, V_{ecp}, provides some kind of average of dynamic properties of the quantum system, so that classical dynamics using V_{ecp} reproduces quantitatively some dynamic results. More precisely, Cao and Voth suggested that classical time correlation functions of position or momentum coordinates, calculated from trajectories generated by the CMD equations, are a well-defined approximation to the Kubo transform of the corresponding quantum time correlation functions.

One appealing characteristic of the CMD equations is their simplicity. However, the derivation of CMD is cumbersome and not easy to understand. From the original CMD derivation,[18] it was not clear why the centroid coordinate should play such a prominent role in the determination of time correlation functions. A more rigorous formulation of CMD was presented by Jang and Voth in 1999.[21–23] The essential step for this improved derivation was the definition of an operator, called the quasi-density operator, whose representation in a position basis corresponds to a fixed centroid path integral. The main result

derived by Jang and Voth was to demonstrate that Kubo transformed time correlation functions of position or momentum operators can be *exactly* represented in terms of averages of operators calculated using the quasi-density operator. The operator formalism presented by Jang and Voth[21] is an essential prerequisite for a sound theoretical formulation of the CMD approximation, and represents a substantial improvement with respect to the original CMD formulation.[18]

The specialized PI concepts that are needed for the definition of CMD, like centroid coordinates, fixed centroid path integrals, and the effective classical potential, cannot be easily translated into physical quantities defined outside the PI formulation. This circumstance is unfortunate, because one who is not familiar with these specialized concepts will have serious difficulties in understanding the physical meaning of CMD and other applications involving centroid coordinates. Paradoxically, the increasing number of these applications over the last 40 years strongly suggest that these concepts have a precise physical significance. This significance should be made clearer if the formulation of CMD were presented without reference to the PI formulation.

One of the main goals of the present chapter is to present a derivation of CMD, and a related improved dynamic approach, by working within the Schrödinger formulation. The Schrödinger formulation of CMD is complementary to the PI formulation and offers some distinct advantages besides. In particular, the Schödinger formulation shows how CMD is related to the time evolution of canonical density operators and also clarifies the relation of CMD to *linear response theory* and the *fluctuation-dissipation theorem*. Both topics are of considerable importance for a full understanding of the CMD approximations. A short account of the Schrödinger formulation of CMD has been presented elsewhere.[24]

This chapter is organized as follows. In Section 2 we review the basic relations that characterize a quantum system in thermodynamic equilibrium. Some auxiliary quantities, that will be used in the Schrödinger formulation of fixed centroid path integrals, are also introduced. The standard PI formulation of fixed centroid path integrals is presented in Section 3, while their Schrödinger formulation is presented in Section 4. The derivation of CMD and a related dynamic approximation is the main goal of Sec. 5. Numerical tests of the capability of these dynamic approximations to treat some exact solvable models are given in Sec. 6. A review of already published CMD simulations is presented in Sec. 7. Some open problems for CMD applications are summarized in Sec. 8. The chapter ends with the conclusions in Sec. 9.

2 Definition of Auxiliary Quantities

For the sake of clarity, we consider a canonical ensemble of independent particles of mass m moving in one dimension. The extension of most of the present study to a many-body problem is straightforward. The Hamiltonian of the particle is assumed to be

$$\hat{H} = \frac{\hat{p}^2}{2m} + V(\hat{x}) \ , \tag{6}$$

where $\hat{x}$, $\hat{p}$, and $V(\hat{x})$ are the position, momentum, and potential energy operators, respectively. The unnormalized canonical density operator of the ensemble of particles is

$$\hat{\rho} = e^{-\beta \hat{H}} \ , \tag{7}$$

where $\beta = (k_B T)^{-1}$ is the inverse temperature and k_B is the Boltzmann constant. The partition function is the trace of the density operator,

$$Z = \mathrm{Tr}[\hat{\rho}] \; . \tag{8}$$

It is convenient to define a normalized density operator, whose trace is unity, by dividing the unnormalized one by its trace. Normalized density operators are represented by a tilde $\tilde{}$,

$$\hat{\tilde{\rho}} = Z^{-1} \hat{\rho} \; . \tag{9}$$

The canonical average of an arbitrary quantum mechanical operator, $\hat{A}$, is the following trace

$$\langle \hat{A} \rangle \equiv \langle \hat{A} \rangle_{\rho} = \mathrm{Tr}[\hat{A} \hat{\tilde{\rho}}] \; . \tag{10}$$

Some auxiliary quantities will be needed for the Schrödinger formulation of fixed centroid path integrals. The first one is the *auxiliary Hamiltonian*, $\hat{H}_a(f, v)$, defined by adding linear terms in $\hat{x}$ and $\hat{p}$ to the Hamiltonian $\hat{H}$

$$\hat{H}_a(f, v) = \hat{H} - f\hat{x} - v\hat{p} \; . \tag{11}$$

The parameter f represents a constant external force acting upon the quantum particle and the parameter v has dimensions of velocity. Note the following equivalence: $\hat{H}_a(0, 0) \equiv \hat{H}$. The *auxiliary canonical density operator*, $\hat{\rho}_a(f, v)$, and the *auxiliary partition function*, $Z_a(f, v)$ are defined using the auxiliary Hamiltonian, $\hat{H}_a(f, v)$ with the help of Eqs. (7) and (8). The average of an operator $\hat{A}$, calculated with the auxiliary density operator, $\hat{\rho}_a(f, v)$, is

$$\langle \hat{A} \rangle_{\rho_a(f,v)} = \mathrm{Tr}[\hat{A} \hat{\tilde{\rho}}_a(f, v)] \; , \tag{12}$$

where the normalized auxiliary canonical density operator is

$$\hat{\tilde{\rho}}_a(f, v) = [Z_a(f, v)]^{-1} \hat{\rho}_a(f, v) \; . \tag{13}$$

3 Definition of Fixed Centroid Path Integrals

In this Section, we present the PI formulation of the canonical density matrix and the definition of fixed centroid path integrals. An important relation between fixed centroid path integrals and the auxiliary canonical density matrix is derived. This relation will provide the starting point for the Schrödinger formulation of fixed centroid path integrals.

3.1 PI Formulation of the Canonical Density Matrix

The position representation of the unnormalized canonical density operator, $\hat{\rho}$, is the matrix

$$\rho(x, x') \equiv \langle x | \hat{\rho} | x' \rangle \; , \tag{14}$$

where $|x\rangle$ is an eigenfunction of the operator $\hat{x}$. The matrix elements $\rho(x, x')$ are *propagators* representing the probability amplitude associated to the movement of the particle

from position x' to x in an Euclidean time $\beta\hbar$. The phase space PI formulation of these matrix elements is[25]

$$\rho(x,x') = \int_{x'}^{x} D[x(u),p(u)]\, e^{-\frac{S[x(u),p(u)]}{\hbar}} \ . \tag{15}$$

$[x(u),p(u)]$ are the position and momentum defining a particle path in phase space. The Euclidean time action is defined by the following functional of the path

$$S[x(u),p(u)] = \int_0^{\beta\hbar} du\, \left\{ \frac{p(u)^2}{2m} + V[x(u)] - ip(u)\dot{x}(u) \right\} \ , \tag{16}$$

where $\dot{x}(u)$ is the derivative of $x(u)$ with respect to u. The integral measure is given by

$$D[x(u),p(u)] = \lim_{N\to\infty} \prod_{k=1}^{N-1} dx_k \prod_{k=0}^{N-1} dp_k \left(\frac{1}{2\pi\hbar}\right)^N \ , \tag{17}$$

where the path $[x(u),p(u)]$ has been discretized in phase space as

$$(x',p_0),(x_1,p_1),(x_2,p_2),...,(x_{N-1},p_{N-1}),(x,p_0) \ . \tag{18}$$

The Euclidean time action in Eq. (16) displays a quadratic dependence on the momentum coordinates $p(u)$. Therefore, all Gaussian integrals in $p(u)$ that appear in Eq. (15) can be evaluated analytically. The resulting path integral is[1,25]

$$\rho(x,x') = \int_{x'}^{x} D_x[x(u)]\, e^{-\frac{S_x[x(u)]}{\hbar}} \ , \tag{19}$$

where the Euclidean time action is now

$$S_x[x(u)] = \int_0^{\beta\hbar} du\, \left\{ \frac{m}{2}\dot{x}(u)^2 + V[x(u)] \right\} \ , \tag{20}$$

and the integral measure is given by

$$D_x[x(u)] = \lim_{N\to\infty} \prod_{k=1}^{N-1} dx_k \left(\frac{mN}{2\pi\beta\hbar^2}\right)^{\frac{N}{2}} \ . \tag{21}$$

3.2 PI Formulation of Constrained Propagators

The *centroid position* and *centroid momentum* of a given path $[x(u),p(u)]$ are defined as the average position and momentum of the path

$$x_c = \frac{1}{\beta\hbar}\int_0^{\beta\hbar} du\, x(u) \ , \tag{22}$$

$$p_c = \frac{1}{\beta\hbar}\int_0^{\beta\hbar} du\, p(u) \ . \tag{23}$$

For the uncountable set of paths contributing to the path integral in Eq. (15), the property of having the same average point x_c and p_c is an equivalence relation that allows us to classify the paths into equivalence classes.[9] Each value of (x_c,p_c) labels a different class

of paths. A *fixed centroid path integral* or *constrained propagator* is defined by a path integral like Eq. (15), that includes only the paths of a given equivalence class (X, P)

$$\sigma(x, x'; X, P) = \int_{x'}^{x} D[x(u), p(u)]\delta(X - x_c)\delta(P - p_c)\, e^{-\frac{S[x(u),p(u)]}{\hbar}} \ , \qquad (24)$$

where δ is the Dirac delta function. The path integral in Eq. (15) can be recovered by integrating over all equivalence classes

$$\rho(x, x') = \int_{-\infty}^{\infty}\int_{-\infty}^{\infty} dX dP \sigma(x, x'; X, P) \ . \qquad (25)$$

It is important to formulate the relationship between fixed centroid path integrals, $\sigma(x, x'; X, P)$, and the auxiliary canonical density matrix, $\rho_a(x, x'; f, v)$. Considering the definition of the Euclidean time action in Eq. (16), one readily derives that the Euclidean time action corresponding to the auxiliary Hamiltonian $\hat{H}_a(f, v)$, is related to that one of the original Hamiltonian, $\hat{H}$, by

$$S_a[x(u), p(u); f, v] = S[x(u), p(u)] - \beta\hbar f X - \beta\hbar v P \ , \qquad (26)$$

where (X, P) are the centroid position and momentum of the path $[x(u), p(u)]$. This result implies that the PI formulation of the auxiliary density matrix can be written as

$$\rho_a(x, x'; f, v) = \int_{x'}^{x} D[x(u), p(u)]\, e^{-\frac{S[x(u),p(u)]}{\hbar}} e^{\beta f X} e^{\beta v P} \ . \qquad (27)$$

Considering the definition of the fixed centroid path integral in Eq. (24), the previous relation can be alternatively written as

$$\rho_a(x, x'; f, v) = \int_{-\infty}^{\infty}\int_{-\infty}^{\infty} dX dP \sigma(x, x'; X, P) e^{\beta f X} e^{\beta v P} \ . \qquad (28)$$

This equation shows that the canonical propagator, $\rho_a(x, x'; f, v)$, and the constrained propagator, $\sigma(x, x'; X, P)$, are related by a two-sided Laplace transform.[26] The variables $(X, \beta f)$ and $(P, \beta v)$ form pairs of conjugate variables in this integral transform. This relation is the essential link to define fixed centroid path integrals within the Schrödinger formulation.

4 The Schrödinger Formulation of Fixed Centroid Path Integrals

We have chosen to present the results of this Section in a way that is formally analogous to the formulation of the Wigner representation of canonical density operators.[27] We recall that with the help of an *integral transform* of the canonical density matrix, $\rho(x, x')$, one defines the Wigner representation, $\rho^W(x, p)$. The coordinates (x, p) of the Wigner matrix defines a phase space, and the statical and dynamic properties of the canonical ensemble can be represented within this phase space.

In this Section, we will define by an integral transform of the auxiliary density operator, $\hat{\rho}_a(f, v)$, a new representation, $\hat{\sigma}(X, P)$. The coordinates (X, P) define a phase space and we will show that the statical and dynamic properties of the canonical ensemble can be represented within this phase space.

Some results of this section have been derived by Jang and Voth using the PI formulation.[21] However, our derivation is presented without reference to the PI formulation and offers new physical insight. A short account of the present derivation has been presented elsewhere.[24]

4.1 Definition of the Static Response Phase Space

As Eq. (28) is valid for arbitrary x and x', one can omit these variables to get a relation between quantum mechanical operators

$$\hat{\rho}_a(f,v) = \int_{-\infty}^{\infty}\int_{-\infty}^{\infty} dXdP\hat{\sigma}(X,P)e^{\beta f X}e^{\beta v P} \ . \tag{29}$$

The auxiliary density operator, $\hat{\rho}_a(f,v)$, is related to the operator $\hat{\sigma}(X,P)$ by a two-sided Laplace transform. This integral transform is an operator relation that can be used as starting point to define $\hat{\sigma}(X,P)$, without referring to the PI formulation.

It is convenient to visualize that the coordinates (X,P) define a phase space associated with the canonical ensemble: The *static response (SR) phase space*. Each phase space point, (X,P), is associated to a quantum mechanical operator, $\hat{\sigma}(X,P)$. The name "SR phase space" has been chosen because the auxiliary density operator $\hat{\rho}_a(f,v)$ obviously depends on the *static response* of the original canonical ensemble to arbitrary linear modifications of its Hamiltonian $\hat{H}$. The SR phase space has interesting properties, in particular for the study of the *linear response* of the canonical ensemble defined by the Hamiltonian $\hat{H}$ (see below).

By taking the trace of the operators in Eq. (29), and considering the linear property of two-sided Laplace transforms, one readily derives

$$Z_a(f,v) = \int_{-\infty}^{\infty}\int_{-\infty}^{\infty} dXdP\ C(X,P)e^{\beta f X}e^{\beta v P} \ , \tag{30}$$

where $C(X,P)$ is the following trace

$$C(X,P) = \mathrm{Tr}[\hat{\sigma}(X,P)] \ . \tag{31}$$

We refer to $C(X,P)$ as the *SR phase space density* associated to the point (X,P). The *SR phase space average* of an arbitrary function, $g(X,P)$, is defined as

$$\{g(X,P)\} = Z^{-1}\int_{-\infty}^{\infty}\int_{-\infty}^{\infty} dXdP\ C(X,P)g(X,P) \ . \tag{32}$$

Note the use of braces $\{...\}$ to represent SR phase space averages. The basic elements of the SR phase space are illustrated in Fig. 1 .

For the formulation of operator averages it is convenient to define a normalized operator

$$\hat{\tilde{\sigma}}(X,P) = [C(X,P)]^{-1}\hat{\sigma}(X,P) \ . \tag{33}$$

We call $\hat{\tilde{\sigma}}(X,P)$ the *generalized SR density operator*. The word *generalized* indicates that $\hat{\tilde{\sigma}}(X,P)$ is a generalization of a true density operator, in the sense that it describes mixed states where the "probabilities", w_n, associated to the eigenfunctions of the operator, may be not only numbers satisfying $0 \leq w_n \leq 1$, but also numbers greater than one and lower than zero (see below). For a true density operator, as $\hat{\tilde{\rho}}(f,v)$, these probabilities are necessarily numbers in the range $0 \leq w_n \leq 1$.

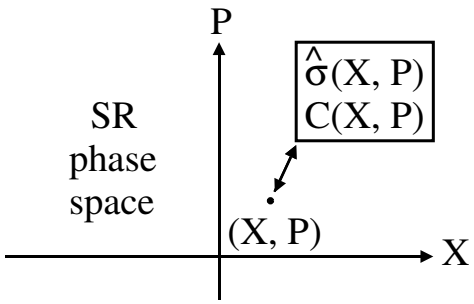

Figure 1. Schematic representation of the SR phase space. Each phase space point (X, P) is associated with a quantum operator, $\hat{\sigma}(X, P)$, whose trace defines the phase space density, $C(X, P)$.

By setting $f = 0$ and $v = 0$ in Eq. (29) and after dividing by Z, one derives the definition of the normalized canonical density operator as a SR phase space average

$$\hat{\bar{\rho}} \equiv \{\hat{\bar{\sigma}}(X, P)\} \; . \tag{34}$$

To avoid confusion in the nomenclature, let us summarize the relationship between the phase space concepts introduced in this section, and fixed centroid path integral concepts, that are currently used in the literature:

- The SR phase space coordinates (X, P) are the centroid position X and momentum P associated to fixed centroid path integrals.

- The position representation of the unnormalized operator, $\hat{\sigma}(X, P)$, corresponds to the fixed centroid path integral given in Eq. (24).

- The normalized operator $\hat{\bar{\sigma}}(X, P)$ is identical to the quasi-density operator defined by Jang and Voth[21] as the inverse two-sided Laplace transform of Eq. (29).

The main advantage of our formulation,[24] with respect to the similar work by Jang and Voth,[21] is that we make explicit use of the integral transform relation in Eq. (29) to derive the properties of the operator $\hat{\bar{\sigma}}(X, P)$. For example, given the dynamic and Bloch equations for the auxiliary canonical density operator, $\hat{\bar{\rho}}_a(f, v)$, Eq. (29) allows us to derive the corresponding transformed equations for $\hat{\bar{\sigma}}(X, P)$.

In the next Subsections, the most important properties of the SR phase space are derived. We focus on the four following topics:

- the dynamic equation for $\hat{\sigma}(X, P)$,

- the Bloch equation for $\hat{\sigma}(X, P)$,

- the formulation of canonical averages as SR phase space averages,

- the formulation of time correlation functions as SR phase space averages.

4.2 Dynamic Equation for the Operator $\hat{\sigma}(X, P)$

The dynamic equation of the auxiliary canonical density operator, $\hat{\rho}_a(f, v)$, evolving in time under the action of the Hamiltonian $\hat{H}$, is

$$i\hbar \frac{\partial \hat{\rho}_a(f,v)}{\partial t} = [\hat{H}, \hat{\rho}_a(f,v)] \ , \tag{35}$$

where $[\hat{H}, \hat{\rho}_a(f, v)]$ is the commutator of the operators inside the square brackets. This relation is the starting point to derive the dynamic equation for $\hat{\sigma}(X, P)$. The time derivative of the two-sided Laplace transform in Eq. (29) is

$$\frac{\partial \hat{\rho}_a(f,v)}{\partial t} = \int_{-\infty}^{\infty}\int_{-\infty}^{\infty} dX dP \frac{\partial \hat{\sigma}(X,P)}{\partial t} e^{\beta f X} e^{\beta v P} \ . \tag{36}$$

By applying (left and right) the Hamiltonian operator $\hat{H}$ to Eq. (29), and taking into account the linear property of the operator $\hat{H}$, one gets

$$\hat{H}\hat{\rho}_a(f,v) = \int_{-\infty}^{\infty}\int_{-\infty}^{\infty} dX dP \hat{H}\hat{\sigma}(X,P) e^{\beta f X} e^{\beta v P} \ , \tag{37}$$

$$\hat{\rho}_a(f,v)\hat{H} = \int_{-\infty}^{\infty}\int_{-\infty}^{\infty} dX dP \hat{\sigma}(X,P)\hat{H} e^{\beta f X} e^{\beta v P} \ . \tag{38}$$

Subtracting the last two Eqs., one derives

$$[\hat{H}, \hat{\rho}_a(f,v)] = \int_{-\infty}^{\infty}\int_{-\infty}^{\infty} dX dP [\hat{H}, \hat{\sigma}(X,P)] e^{\beta f X} e^{\beta v P} \ . \tag{39}$$

The results of Eqs. (35), (36), and (39) imply that the dynamic equation for $\hat{\sigma}(X, P)$ is identical to that one corresponding to a canonical density operator

$$i\hbar \frac{\partial \hat{\sigma}(X,P)}{\partial t} = [\hat{H}, \hat{\sigma}(X,P)] \ . \tag{40}$$

This dynamic equation can be integrated to give

$$\hat{\sigma}(X, P; t) = e^{-i\frac{\hat{H}t}{\hbar}} \hat{\sigma}(X,P) e^{i\frac{\hat{H}t}{\hbar}} \ . \tag{41}$$

By taking the trace of the last equation and considering the cyclic invariance of the trace of a product of operators, one readily derives that the trace, $C(X, P)$, of this operator is a conserved quantity

$$\mathrm{Tr}[\hat{\sigma}(X, P; t)] = \mathrm{Tr}[\hat{\sigma}(X, P)] \ . \tag{42}$$

4.3 Bloch Equation for the Operator $\hat{\sigma}(X, P)$

The Bloch equation, defining the temperature dependence of the operator $\hat{\sigma}(X, P)$, can be derived as the two-sided Laplace transform of the Bloch equation of the auxiliary density operator $\hat{\rho}_a(f, v)$

$$\frac{\partial \hat{\rho}_a(f,v)}{\partial \beta} = -\hat{H}_a(f,v)\hat{\rho}_a(f,v) \ . \tag{43}$$

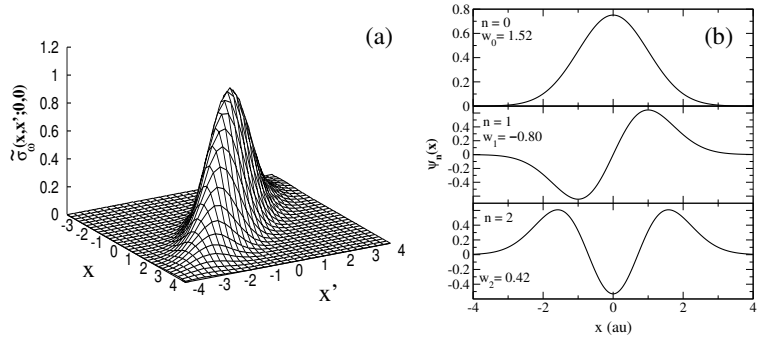

Figure 2. (a) Three-dimensional plot of the SR density matrix $\tilde{\sigma}_\omega(x, x'; 0, 0)$ corresponding to a harmonic oscillator with $m = \omega = 1$ a.u. and $\beta = 2$ a.u.. (b) Eigenfunctions, $\psi_n(x)$, and eigenvalues, w_n, of $\tilde{\sigma}_\omega(x, x'; 0, 0)$ for $n \leq 2$. The eigenfunctions are identical to the energy eigenfunctions of a harmonic oscillator. The eigenvalues form an alternating series of positive and negative real numbers.

This derivation is straightforward and it has been published elsewhere,[28] therefore we present the final result

$$\frac{\partial \hat{\sigma}(X,P)}{\partial \beta} = -\left[\hat{H} + \frac{\hat{x}-X}{\beta}\frac{\partial}{\partial X} + \frac{\hat{p}-P}{\beta}\frac{\partial}{\partial P} - \frac{2}{\beta}\right]\hat{\sigma}(X,P) \tag{44}$$

One interesting point to be stressed here is that this Bloch equation can be solved analytically for the particular case of a harmonic oscillator.[28] The spectral decomposition of the harmonic SR density operator reads

$$\hat{\tilde{\sigma}}_\omega(X,P) = \sum_{n=0}^{\infty} w_n |\psi_n(X,P)\rangle\langle\psi_n(X,P)| \,, \tag{45}$$

where w_n are the eigenvalues and $|\psi_n(X,P)\rangle$ are the eigenvectors of the operator.

At temperature $T = 0$ all eigenvalues are zero except $w_0 = 1$.[28] This result means that $\hat{\tilde{\sigma}}_\omega(X,P)$ is a pure quantum state at $T = 0$. However, at finite temperature ($T > 0$), the eigenvalues w_n form an alternating series of positive and negative real numbers. Then, the operator, $\hat{\tilde{\sigma}}_\omega(X,P)$, is a generalization of a true density operator, in the sense that the "probabilities" or occupation numbers associated to some eigenvectors are allowed to be negative real numbers or even larger that unity. For a harmonic oscillator the eigenvalues w_n satisfy the conditions[28]

$$\sum_{n=0}^{\infty} w_n = 1, \quad |w_n| \leq 2. \tag{46}$$

The SR density matrix associated to the SR phase space point $(0, 0)$,

$$\tilde{\sigma}_\omega(x, x'; 0, 0) = \langle x|\hat{\tilde{\sigma}}_\omega(0,0)|x'\rangle \,, \tag{47}$$

is shown in Fig. 2a. The first eigenfunctions and eigenvalues of this operator are shown in Fig. 2b.

4.4 Formulation of Canonical Averages as SR Phase Space Averages

We want to formulate the SR phase space representation of the canonical average of an arbitrary operator, $\hat{A}$. By applying $\hat{A}$ to Eq. (29) and by taking into account the linear property of quantum mechanical operators, one gets

$$\hat{A}\hat{\rho}_a(f,v) = \int_{-\infty}^{\infty}\int_{-\infty}^{\infty} dXdP\hat{A}\hat{\sigma}(X,P)e^{\beta fX}e^{\beta vP} \; . \tag{48}$$

From the linear property of the two-sided Laplace transform, one derives

$$\mathrm{Tr}[\hat{A}\hat{\rho}_a(f,v)] = \int_{-\infty}^{\infty}\int_{-\infty}^{\infty} dXdP\ \mathrm{Tr}[\hat{A}\hat{\sigma}(X,P)]e^{\beta fX}e^{\beta vP} \; . \tag{49}$$

Dividing both members by $Z_a(f,v)^{-1}$, and multiplying and dividing the integrand by $C(X,P)$, we obtain

$$\langle\hat{A}\rangle_{\rho_a(f,v)} = [Z_a(f,v)]^{-1}\int_{-\infty}^{\infty}\int_{-\infty}^{\infty} dXdP\ C(X,P)\langle\hat{A}\rangle_{\sigma(X,P)}e^{\beta fX}e^{\beta vP} \; , \tag{50}$$

where the average of $\hat{A}$ using the SR density operator is

$$\langle\hat{A}\rangle_{\sigma(X,P)} = \mathrm{Tr}[\hat{A}\hat{\tilde{\sigma}}(X,P)] \; . \tag{51}$$

By setting $f = 0$ and $v = 0$ in Eq. (50), one gets

$$\langle\hat{A}\rangle = \{\langle\hat{A}\rangle_{\sigma(X,P)}\} \; . \tag{52}$$

This relation shows that arbitrary canonical averages can be represented as SR phase space averages.

4.5 Formulation of Time Correlation Functions as SR Phase Space Averages

The *time correlation function* of the position operator $\hat{x}$ and an arbitrary operator $\hat{A}$ is defined by[29]

$$C_{xA}(t) \equiv \langle\hat{x}(0)\hat{A}(t)\rangle = Z^{-1}\mathrm{Tr}[e^{-\beta\hat{H}}\hat{x}(0)\hat{A}(t)] \; , \tag{53}$$

where the Heisenberg operator $\hat{A}(t)$ is

$$\hat{A}(t) = e^{i\frac{\hat{H}t}{\hbar}}\hat{A}e^{-i\frac{\hat{H}t}{\hbar}} \; . \tag{54}$$

The *Kubo transformed time correlation function* is defined as[29]

$$K_{xA}(t) \equiv \langle\hat{x}(0);\hat{A}(t)\rangle = \int_0^{\beta}\frac{d\lambda}{\beta}\langle\hat{x}(-i\lambda\hbar)\hat{A}(t)\rangle \; , \tag{55}$$

where the operator $\hat{x}(-i\lambda\hbar)$ is [see Eq. (54)]

$$\hat{x}(-i\lambda\hbar) = e^{\lambda\hat{H}}\hat{x}e^{-\lambda\hat{H}} \; . \tag{56}$$

The definition in Eq. (55) is written in a form that is not ideal for grasping the physical meaning of Kubo transformed time correlation functions. An alternative definition is based on *linear response theory* and the *fluctuation-dissipation theorem*.[29] We are interested in near-equilibrium states driven by the external force, f. Let us assume that the external

perturbation started to work in the infinite past, i.e., at $t \to -\infty$, when the system with Hamiltonian $\hat{H}_a(f,0)$ was in equilibrium at a certain temperature, i.e., the density matrix was initially canonical, $\hat{\rho}_a(f,0)$. At $t=0$ the external perturbation is set to zero ($f=0$) and then the system evolves in time under the action of the unperturbed Hamiltonian $\hat{H}$. The average of an arbitrary operator $\hat{A}$ at $t>0$ is

$$\langle \hat{A}(t) \rangle_{\rho_a(f,0)} = [Z_a(f,0)]^{-1} \mathrm{Tr}\left[\hat{\rho}_a(f,0)\hat{A}(t)\right] \ , \tag{57}$$

where the time dependence of the Heisenberg operator $\hat{A}(t)$ is determined by the unperturbed Hamiltonian $\hat{H}$ [see Eq. (54)].

The Kubo transformed time correlation function can be defined by the following expression, which is a version of the quantum fluctuation-dissipation theorem[29]

$$\langle \hat{x}(0); \hat{A}(t) \rangle = \frac{1}{\beta} \left[\frac{\partial \langle \hat{A}(t) \rangle_{\rho_a(f,0)}}{\partial f} \right]_{f=0} + \langle \hat{x}(0) \rangle \langle \hat{A}(0) \rangle \ , \tag{58}$$

This expression displays, more clearly than Eq. (55), the physical meaning of Kubo transformed time correlation functions. Note that the definition of the derivative implies

$$\left[\frac{\partial \langle \hat{A}(t) \rangle_{\rho_a(f,0)}}{\partial f} \right]_{f=0} = \lim_{f \to 0} \frac{\langle \hat{A}(t) \rangle_{\rho_a(f,0)} - \langle \hat{A}(0) \rangle}{f} \ , \tag{59}$$

where we have considered that the average of $\hat{A}(t)$ is stationary if the external force vanishes ($f=0$), i.e.,

$$\langle \hat{A}(t) \rangle_{\rho_a(0,0)} \equiv \langle \hat{A}(t) \rangle = \langle \hat{A}(0) \rangle \ . \tag{60}$$

Eqs. (58) and (59) imply that the time dependence of the Kubo transformed function $K_{xA}(t)$ is determined by the time dependence of the average $\langle \hat{A}(t) \rangle_{\rho_a(f,0)}$ for a vanishing small value of f.

Our next goal is to derive the representation of Kubo transformed time correlation functions as SR phase space averages. Note that the derivation of Eq. (50), giving the average, $\langle \hat{A} \rangle_{\rho_a(f,v)}$, as an integral over the SR phase space, is also valid if the operator $\hat{A}$ is substituted by $\hat{A}(t)$. Then, by applying Eq. (50) to the operator $\hat{A}(t)$ and after setting $v=0$ in the resulting expression, one gets

$$\langle \hat{A}(t) \rangle_{\rho_a(f,0)} = [Z_a(f,0)]^{-1} \int_{-\infty}^{\infty} \int_{-\infty}^{\infty} dX dP \ C(X,P) \langle \hat{A}(t) \rangle_{\sigma(X,P)} e^{\beta f X} \ . \tag{61}$$

The derivative of the last expression with respect to f is

$$\frac{\partial \langle \hat{A}(t) \rangle_{\rho_a(f,0)}}{\partial f} = [Z_a(f,0)]^{-1} \, \beta \int_{-\infty}^{\infty} \int_{-\infty}^{\infty} dX dP \ C(X,P) X \langle \hat{A}(t) \rangle_{\sigma(X,P)} e^{\beta f X} - \beta \langle \hat{x}(0) \rangle_{\rho_a(f,0)} \langle \hat{A}(t) \rangle_{\rho_a(f,0)} \tag{62}$$

where the second term comes from the derivative of $[Z_a(f,0)]^{-1}$ with respect to f by noting that

$$Z_a(f,0) = e^{-\beta F_a(f,0)} \ , \tag{63}$$

$$\frac{\partial Z_a(f,0)}{\partial f} = -Z_a(f,0)\beta\frac{\partial F_a(f,0)}{\partial f} = Z_a(f,0)\beta\langle\hat{x}(0)\rangle_{\rho_a(f,0)} \ . \tag{64}$$

$F_a(f,0)$ is the auxiliary free energy. For the particular case that $f = 0$, Eq. (62) reads

$$\left[\frac{\partial\langle\hat{A}(t)\rangle_{\rho_a(f,0)}}{\partial f}\right]_{f=0} = Z^{-1}\beta\int_{-\infty}^{\infty}\int_{-\infty}^{\infty} dX dP\ C(X,P)X\langle\hat{A}(t)\rangle_{\sigma(X,P)} - \beta\langle\hat{x}(0)\rangle\langle\hat{A}(0)\rangle \ , \tag{65}$$

The last equation can be alternatively written as

$$\left[\frac{\partial\langle\hat{A}(t)\rangle_{\rho(f,0)}}{\partial f}\right]_{f=0} = \beta\{X\langle\hat{A}(t)\rangle_{\sigma(X,P)}\} - \beta\langle\hat{x}(0)\rangle\langle\hat{A}(0)\rangle \ . \tag{66}$$

Comparing the last expression with Eq. (58), we see that

$$\langle\hat{x}(0);\hat{A}(t)\rangle \equiv \{X\langle\hat{A}(t)\rangle_{\sigma(X,P)}\} \ , \tag{67}$$

i.e., the Kubo transformed time correlation function $\langle\hat{x}(0);\hat{A}(t)\rangle$ can be expressed as a SR phase space average. An analogous derivation using the auxiliary Hamiltonian $\hat{H}(0,v)$ leads to the result

$$\langle\hat{p}(0);\hat{A}(t)\rangle \equiv \{P\langle\hat{A}(t)\rangle_{\sigma(X,P)}\} \ . \tag{68}$$

Note that these results can not be generalized to the calculation of a correlation function $\langle\hat{B}(0);\hat{A}(t)\rangle$, if the operator $\hat{B}$ is different from $\hat{x}$ or $\hat{p}$.

5 Constrained Time Evolution of the Operator $\hat{\tilde{\sigma}}(X,P)$

We have defined the most important *formal relations* that characterize the SR phase space. Our next goal is the formulation of a *practical approximation* aiming at the calculation of the Kubo transformed time correlation function as a SR phase space average using Eqs. (67) or (68). The dynamic information in these expressions is carried by the average

$$\langle\hat{A}(t)\rangle_{\sigma(X,P)} = \mathrm{Tr}[\hat{A}(t)\hat{\tilde{\sigma}}(X,P)] = \mathrm{Tr}[\hat{A}\hat{\tilde{\sigma}}(X,P;t)] \ , \tag{69}$$

where

$$\hat{\tilde{\sigma}}(X,P;t) = [C(X,P)]^{-1}\hat{\sigma}(X,P;t) \ , \tag{70}$$

and $\hat{A}(t)$ and $\hat{\sigma}(X,P;t)$ were defined by Eqs. (41) and (54), respectively.

The exact calculation of $\langle\hat{A}(t)\rangle_{\sigma(X,P)}$ implies [see Eq. (69] the determination of the time evolution of the SR density operator associated to (X,P)

$$\hat{\tilde{\sigma}}(X,P) \ \text{(time =0)} \quad \longrightarrow \quad \hat{\tilde{\sigma}}(X,P;t) \ \text{(time =t)} \ . \tag{71}$$

The computation of this time evolution is, for a general quantum system, a difficult problem. Moreover, the calculation of a SR phase space average implies solving this difficult problem for a set of operators associated with different points (X,P). The only practical route to undertake this calculation lies on the formulation of an approximate dynamics for the SR density operator. CMD should be understood as an approximate dynamics for the SR density operator. One clear reason for the difficulty in understanding the original CMD

formulation is that CMD was formulated in 1994,[18] while the SR density operator was first defined in 1999.[21,24] In this section, an approximate dynamics for the SR density operator is presented by following these steps:

- discussion of a factorization property of the SR density matrix
- formulation of a *variational constrained dynamics* for the SR density operator,
- study of the harmonic and high temperature limits of the dynamic approximation.

5.1 Factorization Property of the Matrix Elements $\sigma(x, x'; X, P)$

The position representation of the SR density operator has a factorization property, that is valid if the Hamiltonian $\hat{H}$ depends quadratically on the momentum operator $\hat{p}$. The derivation has been published elsewhere,[21,28] the final result is that $\sigma(x, x'; X, P)$ factorizes into X- and P-dependent factors

$$\sigma(x, x'; X, P) = \sigma_X(x, x'; X)\sigma_P(x, x'; P) \; . \tag{72}$$

The P-dependent factor is

$$\sigma_P(x, x'; P) = \left(\frac{\beta}{2\pi m}\right)^{\frac{1}{2}} e^{-\frac{\beta P^2}{2m}} e^{\frac{m(x-x')^2}{2\beta\hbar^2}} e^{i\frac{P(x-x')}{\hbar}} \; . \tag{73}$$

The X-dependent factor, $\sigma_X(x, x'; X)$ is the position representation of the operator $\hat{\sigma}_X(X)$, that is defined as

$$\hat{\sigma}_X(X) = \int_{-\infty}^{\infty} dP \hat{\sigma}(X, P) \; . \tag{74}$$

The matrix elements, $\sigma_X(x, x'; X)$, represent constrained propagators whose PI representation is the following fixed centroid path integral

$$\sigma_X(x, x'; X) = \int_{x'}^{x} D_x[x(u)]\delta(X - x_c)\, e^{-\frac{S_x[x(u)]}{\hbar}} \; . \tag{75}$$

The diagonal elements $\sigma_P(x, x; P)$ are [see Eq. (73)], a constant independent of x. This fact implies that the trace of $\sigma(x, x'; X, P)$ factorizes also into X- and P-dependent terms. Using Eq. (72) to calculate this trace, one gets

$$C(X, P) = \int_{-\infty}^{\infty} dx \sigma_X(x, x; X)\sigma_P(x, x; P) \; , \tag{76}$$

$$C(X, P) = C_P(P) \int_{-\infty}^{\infty} dx \sigma_X(x, x; X) \equiv C_P(P)C_X(X) \; . \tag{77}$$

$C_P(P)$ is the *momentum density* in the SR phase space

$$C_P(P) \equiv \sigma_P(x, x; P) = \left(\frac{\beta}{2\pi m}\right)^{\frac{1}{2}} e^{-\frac{\beta P^2}{2m}} \; , \tag{78}$$

which has the form of a *classical momentum distribution*. $C_X(X)$ is the trace of the operator $\hat{\sigma}_X(X)$, and it is the *position density* in the SR phase space. This density is used to define the effective classical potential, $V_{ecp}(X)$, as

$$C_X(X) = \left(\frac{m}{2\pi\hbar^2\beta}\right)^{\frac{1}{2}} \; e^{-\beta V_{ecp}(X)} \; . \tag{79}$$

Other property derived from the fact that $\sigma_P(x,x;P)$ does not depend on x is the following: The averages $\langle\hat{A}\rangle_{\sigma(X,P)}$ of operators defined as arbitrary functions of $\hat{x}$ do not depend on the variable P. For example, the *mean force*, $f_m(X)$, is the average of the force operator, $\hat{f}_r$,

$$\langle\hat{f}_r\rangle_{\sigma(X,P)} = Z^{-1}\int_{-\infty}^{\infty} dx \left[-\frac{dV(x)}{dx}\right]\sigma_X(x,x;X) \equiv f_m(X) \; . \tag{80}$$

f_m is a function of X but not of P. Another important average is the dispersion of the position operator $\hat{x}$

$$\delta x^2(X) = \langle\hat{x}^2\rangle_{\sigma(X,P)} - \left[\langle\hat{x}\rangle_{\sigma(X,P)}\right]^2 \; , \tag{81}$$

that does not depend on the coordinate P. We note that

$$\langle\hat{x}\rangle_{\sigma(X,P)} = X \tag{82}$$

5.2 A Variational Constrained Dynamic Approximation

An approximate dynamics for the operator $\hat{\tilde{\sigma}}(X,P)$ is defined by the following two conditions:

- (i) *Constrained dynamics*: The dynamic state at an arbitrary time t is constrained to be a SR density operator, $\hat{\tilde{\sigma}}(X,P)$,

  $$\hat{\tilde{\sigma}}(X,P;t) \approx \hat{\tilde{\sigma}}(X(t),P(t)) \; . \tag{83}$$

  The constrained time evolution of $\hat{\tilde{\sigma}}(X,P;t)$ is then characterized by a trajectory $[X(t),P(t)]$ in the SR phase space. A representation of the constrained dynamics is given in Fig. 3.

- (ii) *Variational short time approximation*: The constrained dynamic equations are derived from the Gauss *principle of least constraint*, i.e., from the condition that the difference, in a least square sense, between the exact and constrained short time dynamics of $\hat{\tilde{\sigma}}(X,P)$ is minimum.

The derivation of the variational short time approximation is done in the position representation. The algebra is straightforward, but rather lengthy. Therefore, we summarize the main steps of the derivation:

(1) The exact (e) time derivative of the matrix elements $\rho_a(x,x';f,v)$ is derived using the time dependent Schrödinger equation. The result is

$$\left[\frac{\partial\rho_a(x,x';f,v)}{\partial t}\right]_e = \left[\frac{f(x-x')}{i\hbar} - v\left(\frac{\partial}{\partial x}+\frac{\partial}{\partial x'}\right)\right]\rho_a(x,x';f,v) \; . \tag{84}$$

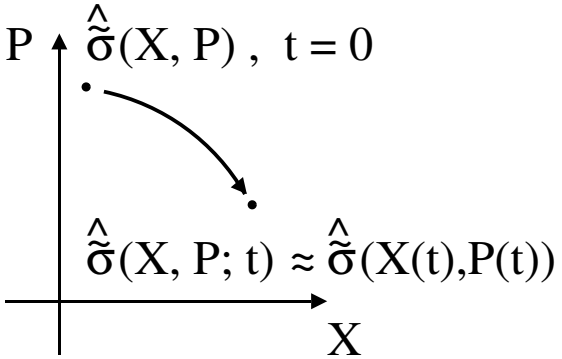

Figure 3. Schematic picture of the constrained dynamics for the operator $\hat{\tilde{\sigma}}(X,P)$, defined at $t = 0$. The dynamic state at time t, $\hat{\tilde{\sigma}}(X,P;t)$, is constrained to be a SR density operator, $\hat{\tilde{\sigma}}(X(t),P(t))$. The arrow represents the trajectory $(X(t), P(t))$ that characterizes the constrained dynamics from $t = 0$ to time t.

(2) The exact time derivative of the matrix elements $\tilde{\sigma}(x,x';X,P)$ is derived with the help of the two-sided Laplace relation between $\rho_a(x,x';f,v)$ and $\sigma(x,x';X,P)$ [see Eq. (28)]. The result is

$$\left[\frac{\partial\tilde{\sigma}(x,x';X,P)}{\partial t}\right]_e = \left[i\left(\frac{x-x'}{\beta\hbar}\right)\left(\frac{\partial}{\partial X}+\frac{\partial}{\partial x}+\frac{\partial}{\partial x'}\right)-\frac{P}{m}\left(\frac{\partial}{\partial x}+\frac{\partial}{\partial x'}\right)\right]\tilde{\sigma}(x,x';X,P)\,. \quad (85)$$

(3) The constrained (c) dynamic equation for $\tilde{\sigma}(x,x';X,P)$ is formulated according to condition (i)

$$\left[\frac{\partial\tilde{\sigma}(x,x';X,P)}{\partial t}\right]_c = \frac{\partial\tilde{\sigma}(x,x';X,P)}{\partial X}\dot{X}+\frac{\partial\tilde{\sigma}(x,x';X,P)}{\partial P}\dot{P}\,. \quad (86)$$

where

$$\dot{X}=\frac{dX}{dt}\quad ;\dot{P}=\frac{dP}{dt}\,. \quad (87)$$

(4) The variational short time approximation is derived from minimizing, with respect to $\dot{X}$ and $\dot{P}$, the following function

$$\mathcal{I}(\dot{X},\dot{P})=\int_{-\infty}^{\infty}\int_{-\infty}^{\infty}dxdx'\left|\left[\frac{\partial\tilde{\sigma}(x,x';X,P)}{\partial t}\right]_e-\left[\frac{\partial\tilde{\sigma}(x,x';X,P)}{\partial t}\right]_c\right|^2\,, \quad (88)$$

where $|...|$ indicates the modulus of a complex number.

(5) The minimization results in the following set of equations that define the constrained dynamics

$$\dot{X}=-\frac{P}{m}\frac{x_1(X,P)}{x_2(X,P)}\,, \quad (89)$$

$$\dot{P} = \frac{p_1(X,P)}{p_2(X,P)} \; . \tag{90}$$

The functions $x_1(X,P)$ and $x_2(X,P)$ are defined by the following integrals, where the shorthand notation, $\sigma_X \equiv \sigma_X(x,x';X)$, $\sigma \equiv \sigma(x,x';X,P)$, and $f_m \equiv f_m(X)$, has been used

$$x_1(X,P) = \int_{-\infty}^{\infty}\int_{-\infty}^{\infty} dxdx'|\sigma|^2 \left(\frac{\partial \ln \sigma_X}{\partial x} + \frac{\partial \ln \sigma_X}{\partial x'}\right)\left(\frac{\partial \ln \sigma_X}{\partial X} - \beta f_m\right) , \tag{91}$$

$$x_2(X,P) = \int_{-\infty}^{\infty}\int_{-\infty}^{\infty} dxdx'|\sigma|^2 \left(\frac{\partial \ln \sigma_X}{\partial X} - \beta f_m\right)^2 . \tag{92}$$

The functions $p_1(X,P)$ and $p_2(X,P)$ are defined by

$$p_1(X,P) = \int_{-\infty}^{\infty}\int_{-\infty}^{\infty} dxdx'|\sigma|^2 (x-x')^2 \frac{1}{\beta}\left(\frac{\partial \ln \sigma_X}{\partial X} + \frac{\partial \ln \sigma_X}{\partial x} + \frac{\partial \ln \sigma_X}{\partial x'}\right) , \tag{93}$$

$$p_2(X,P) = \int_{-\infty}^{\infty}\int_{-\infty}^{\infty} dxdx'|\sigma|^2 (x-x')^2 \; . \tag{94}$$

The variational equations for the constrained dynamics imply the determination of the diagonal and off diagonal elements of the matrix $\sigma(x,x';X,P)$, a cumbersome computational task. Therefore, we will introduce an additional approximation to simplify the variational equations.

5.3 The RMD Approximation

The following *factorization approximation* is applied to simplify the variational equations

$$|\sigma(x,x';X,P)|^2 \approx \sigma(x,x;X,P)\sigma(x',x';X,P) \; . \tag{95}$$

This relation is *exact* for a pure state. E.g., if $\sigma(x,x')$ denotes a pure state, then

$$|\sigma(x,x')|^2 = |\langle x|\psi\rangle\langle\psi|x'\rangle|^2 = \sigma(x,x)\sigma(x',x') \; . \tag{96}$$

We recall that the SR density operator is a pure state only at temperature $T = 0$.[31,32] Therefore, the use of the factorization approximation implies that the variational character of the dynamic equations is lost, except in the limit $T = 0$. The computational advantage of this approximation is that only the diagonal elements of the SR density matrix are needed. We define the function $\phi(x;X)$ as the square root of these diagonal elements

$$\phi(x;X) = [\tilde{\sigma}(x,x;X,P)]^{1/2} \equiv [\tilde{\sigma}_X(x,x;X)]^{1/2} \; . \tag{97}$$

Applying the factorization approximation to the variational equations in Eqs. (89) and (90), one gets

$$\dot{X} = \frac{P}{m}\gamma(X) \; , \tag{98}$$

$$\dot{P} = f_m(X) + \nu(X) \; . \tag{99}$$

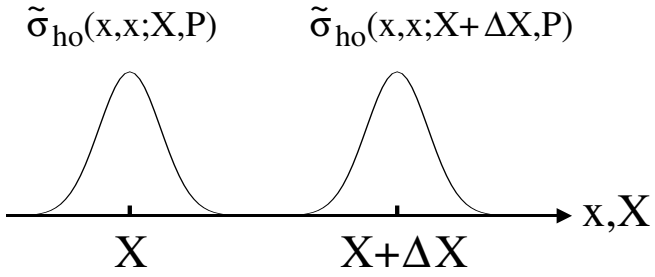

Figure 4. Schematic representation of the translational symmetry of the diagonal elements of the SR density matrix, $\tilde{\sigma}_{ho}(x,x;X,P)$. The diagonal elements associated to two SR phase space positions, X and $X+\Delta X$, are functions of x that differ by an overall translation. This result is valid for a harmonic oscillator at arbitrary temperature and for an arbitrary potential in the high temperature limit.

This dynamic approximation is called the *constrained response matrix dynamics* (RMD). The function $\gamma(X)$ represents a correction factor for the particle mass in the constrained dynamics. It is defined as

$$\gamma(X) = -\frac{\gamma_1(X)}{\gamma_2(X)} \,, \tag{100}$$

$$\gamma_1(X) = \int_{-\infty}^{\infty} dx \frac{\partial\phi(x;X)}{\partial X}\frac{\partial\phi(x;X)}{\partial x} \,, \tag{101}$$

$$\gamma_2(X) = \int_{-\infty}^{\infty} dx \left[\frac{\partial\phi(x;X)}{\partial X}\right]^2 . \tag{102}$$

The function $\nu(X)$ is a temperature dependent correction term for the mean force $f_m(X)$,

$$\nu(X) = \frac{k_B T}{2}\frac{\partial \ln\left[\delta x^2(X)\right]}{\partial X} \,. \tag{103}$$

Note that $\nu(X)$ vanishes at temperature $T = 0$ and that $\delta x^2(X)$ is the dispersion of the operator $\hat{x}$ defined in Eq. (81).

5.4 The Harmonic and High Temperature Limits of the RMD Approximation

Let us apply the RMD equations to a harmonic oscillator (ho) at arbitrary temperature and to the high temperature limit of an arbitrary potential. For these two cases, the diagonal elements of the SR density matrix satisfy the following equation[28]

$$\tilde{\sigma}_{ho}(x,x;X+\Delta X,P) = \tilde{\sigma}_{ho}(x-\Delta X, x-\Delta X;X,P) \,. \tag{104}$$

This relation means that the diagonal elements of the SR density matrix associated to the phase space points (X,P) and $(X+\Delta X,P)$ are identical, apart from an overall translation by ΔX (see Fig 4). Thus, the function $\phi_{ho}(x;X)$, defined in Eq. (97), satisfies the condition

$$\phi_{ho}(x;X+\Delta X) = \phi_{ho}(x-\Delta X;X) \,. \tag{105}$$

This relation can be rewritten using a Taylor expansion of the l.h.s. around X and of the r.h.s. around x. The result, to first order in both Δx and ΔX, is

$$\phi_{ho}(x;X) + \Delta X \frac{\partial \phi_{ho}(x;X)}{\partial X} = \phi_{ho}(x;X) - \Delta X \frac{\partial \phi_{ho}(x;X)}{\partial x} \; . \tag{106}$$

The last equation implies that

$$\frac{\partial \phi_{ho}(x;X)}{\partial X} = -\frac{\partial \phi_{ho}(x;X)}{\partial x} \; . \tag{107}$$

By introducing this result in the definition of $\gamma(X)$ in Eq. (100), one gets

$$\gamma_{ho}(X) = 1 \; . \tag{108}$$

It is also easy to show that

$$\nu_{ho}(X) = 0 \; , \tag{109}$$

as Eq. (105) implies that the dispersion $\delta x^2(X)$ is a constant independent of the coordinate X.

The previous conditions ($\gamma_{ho} = 1$, $\nu_{ho} = 0$) imply that the RMD equations become identical to CMD in the cases where CMD is known to be exact, i.e., for a harmonic oscillator at arbitrary temperature and for an arbitrary potential in the high temperature limit. In the numerical test examples of the following Section, we will see that the correction factors $\gamma(X)$ and $\nu(X)$ have little influence in the resulting dynamics (except in the study of quantum tunneling at temperature $T = 0$). Thus, for practical purposes RMD produces nearly the same dynamic results as CMD and then our derivation of RMD provides new insight into the physical meaning of CMD.

Let us summarize several properties of the RMD and CMD equations:

- At temperature $T = 0$ the RMD approximation is a variational approximation. CMD is, like RMD, a constrained dynamics but it is not a variational approximation. Then, we expect that RMD will provide more accurate results than CMD at temperature $T = 0$.

- At any finite temperature the RMD approximation is not variational, because it includes the factorization approximation given in Eq. (95). One expects that the quality of the RMD and CMD results *decreases* as the temperature increases above $T = 0$, i.e., as the temperature deviates from the variational $T = 0$ limit.

- However, in the high temperature limit, RMD and CMD go over the correct classical limit. Therefore, above some unspecified temperature, the quality of the RMD and CMD results should *increase* as the temperature increases towards the classical limit.

- CMD can be derived from RMD as a harmonic or high temperature limit.

- If $\gamma(X) \neq 1$ or $\nu_{ho}(X) \neq 0$ the RMD equations generate a non-Hamiltonian SR phase space dynamics; i.e., they imply a nonzero phase space compressibility

$$\frac{d}{dt} C[X(t), P(t)] \neq 0 \; . \tag{110}$$

  CMD always conserves the SR phase space probability.

6 Numerical Test on Model Systems

As we stated in the introduction, the capability of CMD (and also RMD) to describe real time quantum dynamics rest on the assumption that the effective classical potential, V_{ecp}, represents some kind of realistic average of dynamic properties. In this Section we apply the CMD and RMD approximations to the study of simple problems that can be solve exactly by mean of numerical techniques.

The main questions to be addressed are:

- In which cases does V_{ecp} carry an accurate dynamic information?
- How does the RMD approximation compare to CMD?

6.1 The Zero Temperature Limit of CMD and RMD

We consider the quantum dynamics of a particle of mass $m = 16$ a.u. moving either on a double-well potential (V_{dw}) or on a quartic potential (V_q), defined as

$$V_{dw}(x) = \frac{1}{4}(x^2 - 1)^2 \ , \tag{111}$$

$$V_q(x) = 2.2015x^4 \ , \tag{112}$$

where x is expressed in a.u.. The V_{ecp} has the following simple physical meaning at temperature $T = 0$:[31,32] It is related to the ground state energy, $E_0(f)$, of the auxiliary Hamiltonian, $\hat{H}_a(f, 0)$,

$$\hat{H}_a(f, 0)|\phi_0(f)\rangle = E_0(f)|\phi_0(f)\rangle \ . \tag{113}$$

$|\phi_0(f)\rangle$ is the ground state of $\hat{H}_a(f, 0)$. The relation between $V_{ecp}(X)$ and $E_0(f)$ has the form of a Legendre transform

$$V_{ecp}(X) = E_0(f) + fX \ , \tag{114}$$

where the centroid position X is the average of the position operator $\hat{x}$

$$X = \langle\phi_0(f)|\hat{x}|\phi_0(f)\rangle = -\frac{dE_0(f)}{df} \ . \tag{115}$$

The calculation of V_{ecp} at $T = 0$, can be done by solving numerically, for a set of values of the parameter f, the time independent Schrödinger equation for the Hamiltonian $\hat{H}_a(f, 0)$. The function V_{ecp} for the studied model potentials are shown in Fig. 5 as continuous lines. The dotted lines are harmonic approximations at the potential minimum located at $X = 0$.

At temperature $T = 0$, the SR density operators associated to the SR phase space points $(X, 0)$ are pure states identical to the kets $|\phi_o(f)\rangle$.[31,32] The centroid position X and the force parameter f are related by Eq. (115). Thus, the RMD and CMD approximations are wave packets dynamics in this $T = 0$ limit. The difference between both approaches is determined by the deviation from unity of the RMD parameter $\gamma(X)$ that appears in Eq. (98). The functions $\gamma(X)$ for the the two studied model potentials are shown in Fig. 6. The deviation of $\gamma(X)$ from unity is appreciable for V_{dw}, but small for V_q.

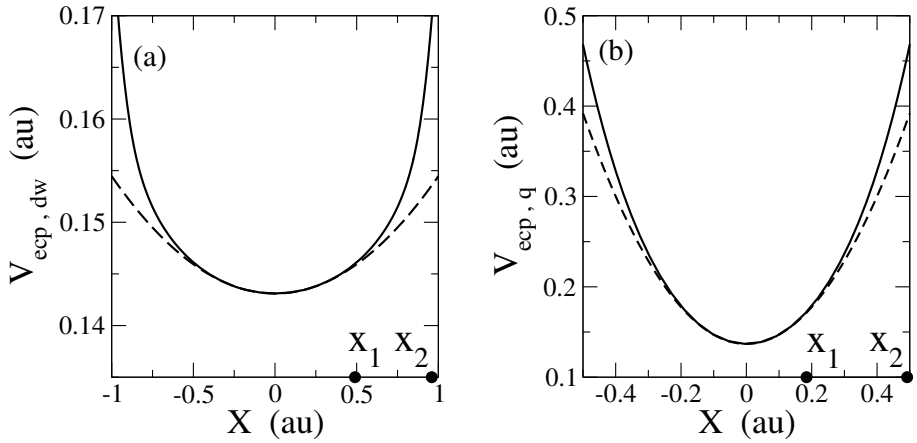

Figure 5. (a) Effective classical potential at temperature $T = 0$ corresponding the double-well potential V_{dw}. The dotted line represents a harmonic approximation around the minimum at $X = 0$. The two positions (X_1 and X_2), marked as filled circles, define two initial ($t = 0$) states used in the dynamic study. (b) The same information is provided for the quartic potential V_q.

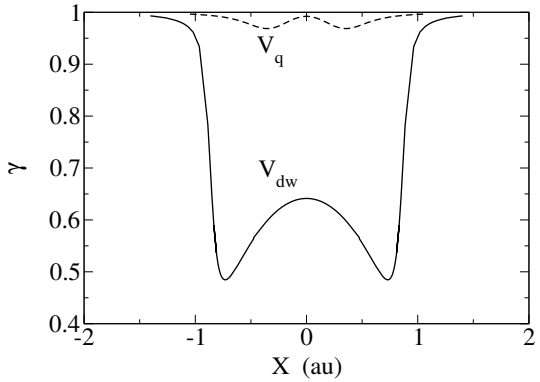

Figure 6. (a) Parameter $\gamma(X)$ for the two studied model potentials at $T = 0$.

For the potential V_{dw}, we study the dynamics of two different initial states corresponding to the SR density operators associated to the points $(X_1, 0)$ and $(X_2, 0)$. The coordinates X_1 and X_2 are shown in Fig. 5a. The coordinate X_1 belongs to a region where V_{ecp} is well described by a harmonic approximation (dotted line in Fig. 5a), while at position X_2, V_{ecp} deviates clearly from the harmonic limit. The exact phase space trajectory $[X(t), P(t)]$ corresponding to a given initial state, $\hat{\tilde{\sigma}}(X, P)$, is determined by the following averages

$$X(t) = \langle \hat{x}(t) \rangle_{\sigma(X,P)} \ , \tag{116}$$

$$P(t) = \langle \hat{p}(t) \rangle_{\sigma(X,P)} \ . \tag{117}$$

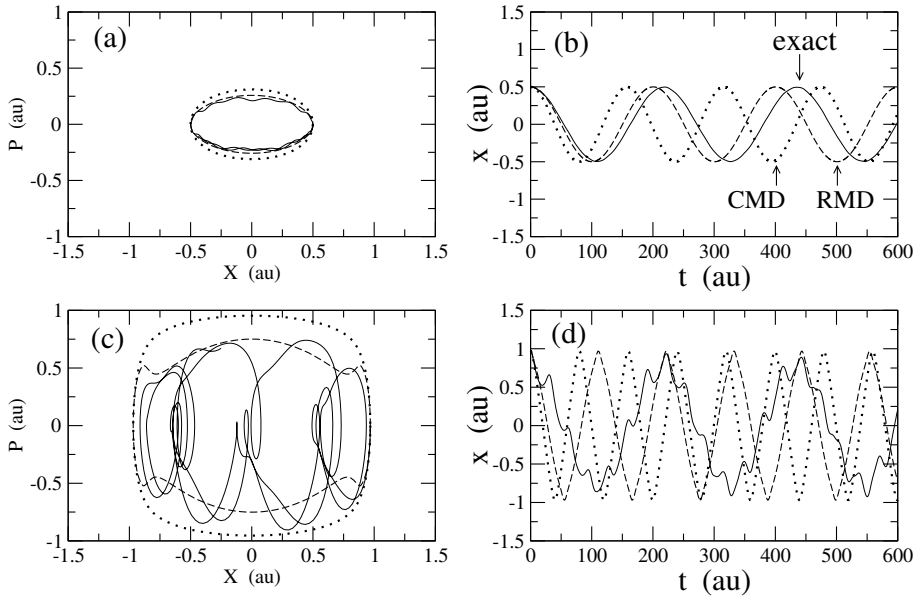

Figure 7. (a) Phase space trajectory for the SR density operator associated to the point $(X_1, 0)$ at time $t = 0$. (b) The average $X(t)$ for SR density operator associated to $(X_1, 0)$ at $t = 0$. (c) Phase space trajectory for the SR density operator associated to the point $(X_2, 0)$ at time $t = 0$. (d) The average $X(t)$ for SR density operator associated to $(X_2, 0)$ at $t = 0$. In the four panels (a)-(d), the exact results are shown by continuous lines, the RMD results by dashed lines, and the CMD results by dotted line. The results corresponds to the double-well model potential, V_{dw}.

The exact phase space trajectories corresponding to the initial states associated to $(X_1, 0)$ and $(X_2, 0)$ are compared in Figs. 7a and 7c with the results derived from the RMD and CMD approximations. The exact result for $X(t)$ is compared to the RMD and CMD expectations in Figs. 7b and 7d. The RMD approximation provides better results than the CMD approximation for the phase space trajectory $[X(t), P(t)]$ and also for the frequency of the oscillation in $X(t)$. The main effect of the factor $\gamma(X)$ in the RMD equations, is the slowing down of this frequency, when compared to the CMD results. The improved RMD results are consequence of its variational character at $T = 0$, a property not shared by CMD.

We observe that the RMD and CMD results derived for the initial state given by $(X_1, 0)$ are more accurate that those one derived for $(X_2, 0)$. This behavior can be rationalized in terms of the dynamical information carried out by the effective classical potential. The initial state defined by $(X_2, 0)$ explores a larger X region along its dynamic evolution than the initial state defined by $(X_1, 0)$, as it is seen by comparing Figs. 7a and 7c. The anharmonicity of V_{ecp} (see Fig. 5) causes that the frequency of the time oscillations in $X(t)$ increases for the initial state defined by $(X_2, 0)$ with respect the result obtained for $(X_1, 0)$ (see Figs. 7b and 7d). This anharmonic effect in V_{ecp} is an *unphysical dynamic result*, because the exact $X(t)$ does not display any change in the oscillation frequency as a function of the initial state. The exact result for $X(t)$ shows that the main dynamic effect associated

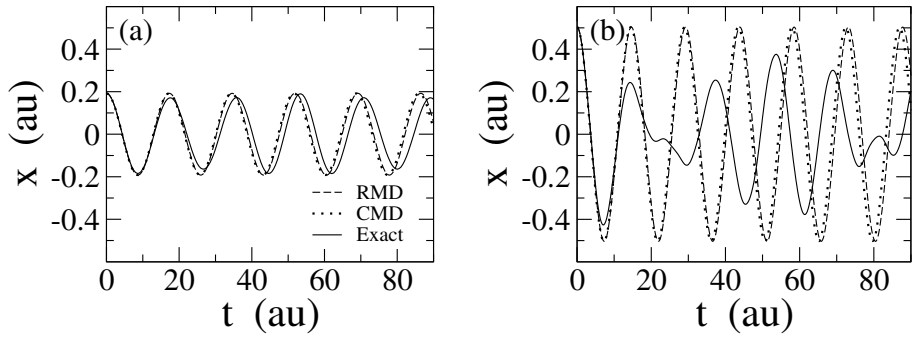

Figure 8. (a) The function $X(t)$ for a initial state defined by the SR density operator associated to the phase state point $(X_1, 0)$. The exact result is compared to the constrained dynamic approximations (RMD and CMD). (b) Exact, RMD, and CMD results for $X(t)$ for an initial state defined by $(X_2, 0)$. The meaning of the plotted lines is the same as for the panel (a). The results correspond to the quartic potential, V_q. Note that the RMD and CMD results are nearly identical.

to the change in the initial condition is a coherent superposition of two different frequencies. Both RMD and CMD are completely unable to reproduce this coherent superposition of frequencies. The final conclusion is that the most meaningful dynamic information of V_{ecp} is contained only in the *harmonic region* around the potential energy minimum at $X = 0$ (see Fig. 5), and that the *anharmonic region* of V_{ecp} provides unphysical dynamic information.

In Fig. 8, we compare the exact result for $X(t)$ with those derived from the RMD and CMD approximations for the quartic potential V_q. We have considered two different initial states defined by the SR density operators associated to the points $(X_1, 0)$ and $(X_2, 0)$, The values X_1 and X_2 are shown in Fig. 5b. We find that for the quartic potential, V_q, the RMD and CMD results are, for practical purposes, indistinguishable. The constrained dynamic approximations (CMD, RMD) are more accurate for the initial state defined by $(X_1, 0)$, when the function $X(t)$ is characterized by oscillations with a unique frequency (see Fig. 8a). For the initial state defined by $(X_2, 0)$, the exact time evolution of $X(t)$ displays a coherent superposition of different frequencies. Again, we find that both RMD and CMD are unable to reproduce this coherent superposition (see Fig. 8b). The main change observed in the CMD and RMD results as a function of the initial condition is an increase in the frequency of the oscillations of $X(t)$. Again, the conclusion to be drawn is that the relevant dynamic information of V_{ecp} at $T = 0$ is reduced to the harmonic part of the potential around the energy minimum, The anharmonic region of V_{ecp} leads to unphysical results in the CMD and RMD approximations.

6.2 Finite Temperature CMD and RMD Results

We present some results for the time correlation function of the position operator at different temperatures

$$C(t) = \langle \hat{x}(0)\hat{x}(t) \rangle = Z^{-1} \mathrm{Tr}[e^{-\beta \hat{H}} \hat{x} e^{i\frac{\hat{H}t}{\hbar}} \hat{x} e^{-i\frac{\hat{H}t}{\hbar}}] \, . \tag{118}$$

Several general properties of quantum time correlation functions can be readily derived by writing them in a basis of eigenfunctions of the Hamiltonian. Thus, $C(t)$ can be shown to be a *complex* function of t.

$$C(t) = C^R(t) + iC^I(t) \ , \tag{119}$$

The corresponding Kubo transformed correlation function, $K(t)$, is a *real* function of t. By defining the Fourier transform of $K(t)$ as

$$\overline{K}(\omega) = \frac{1}{\sqrt{2\pi}} \int_{-\infty}^{\infty} dt K(t) e^{-i\omega t} \ , \tag{120}$$

one can readily show that[18,29,30]

$$\overline{C}^R(\omega) = \frac{\beta\hbar\omega}{2} \coth\left(\frac{\beta\hbar\omega}{2}\right) \overline{K}(\omega) \ , \tag{121}$$

$$i\overline{C}^I(\omega) = \frac{\beta\hbar\omega}{2} \overline{K}(\omega) \ , \tag{122}$$

where $\overline{C}^R(\omega)$ and $\overline{C}^I(\omega)$ are the Fourier transforms of $C^R(t)$ and $C^I(t)$, respectively.

The real part, $C^R(t)$, of the time correlation function of the position operator has been studied for the quartic potential, V_q, at three different temperatures ($T_a = 0.03$, $T_b = 0.14$, and $T_c = 0.5$ $a.u.$). The energy difference between the first excited state and the ground state amounts to $\Delta E = 0.35$ a.u.. Thus, at the two lowest studied temperatures, T_a and T_b, one expects that the time correlation function will be mainly dominated by ground state dynamics, while at T_c one expects dynamic contributions from higher excited states. The exact $C^R(t)$ curves are shown in Fig. 9 by continuous lines. The results corresponding to the CMD (dotted line) and RMD (dashed line) approximations are also displayed in Fig. 9. The first conclusion from these data is that CMD and RMD provide nearly indistinguishable results at all temperatures. The second conclusion is that the time correlation function derived by either CMD or RMD decays to zero too fast as temperature increases. Comparing the CMD results at T_a and T_b, we note that at T_b the time correlation has decayed to zero at times larger than about $t = 40$ a.u.. This is clearly an unphysical behavior related to the anharmonicity of the effective classical potential. Our previous conclusion derived at temperature $T = 0$, that only the harmonic region of V_{ecp} carries meaningful dynamic information seems to be also true at *low enough temperatures*. From the data in Fig. 9, and also from other published numerical work,[32–34,22] one can establish a temperature range

$$k_b T \lesssim \frac{\Delta E}{4} \ , \tag{123}$$

where CMD provides the most realistic results for low temperature quantum dynamics. At temperatures above this range the quality of the CMD results *decreases*. This fact is clearly seen in Fig. 9 by comparing the CMD results at T_a and T_b. The CMD results at T_a are a better approximation to the exact data at T_b, that the CMD results derived at T_b (see Fig. 10). Note that $T_a \approx \frac{\Delta E}{12}$ is in the range defined by Eq. (123), while $T_b \approx \frac{\Delta E}{2}$ is outside this range.

As the temperature increases above the low temperature range defined in Eq. (123), e.g., for the temperatures T_b and T_c in Fig. 9, the CMD data are accurate only for short

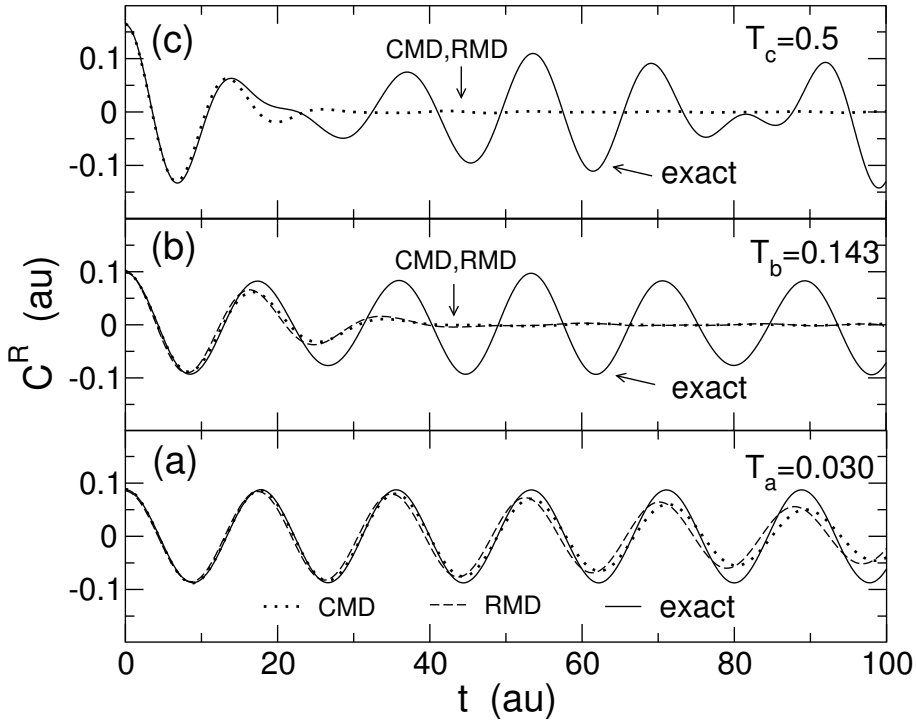

Figure 9. Real part, $C^R(t)$, of the time correlation function of the position operator as calculated for the model potential V_q. The exact results are compared to the CMD and RMD approximations. The CMD and RMD curves are nearly identical. Three temperatures were analyzed: (a) $T = 0.03$ au; (b) $T = 0.143$ au; (c) $T = 0.5$ a.u..

times. The value, t_m, defining the upper time where CMD is accurate should increase with temperature, because t_m becomes eventually infinity in the high temperature limit when CMD becomes exact. An interesting point should be to study how the time t_m depends on temperature.

Other numerical investigations comparing CMD and exact results for position time correlation functions has been published by Krilov and Berne[34], Jang and Voth[22], and Cao and Voth[18,19]. Let us summarize the main conclusions of our numerical investigation at low temperature, that should be applicable to vibrational problems in molecules, solids, impurities in solids, etc.

- The RMD approximation provides results nearly identical to CMD, except in the study of quantum tunneling, where the RMD approximation provides improved results.
- There is a low temperature region, defined as a function of the energy difference between the first excited and ground states [see Eq.(123)], where the significant dynamic information of V_{ecp} is the curvature of the potential around its energy minimum. Long time dynamics derived in this low temperature region by CMD is realistic.
- At temperatures above this low temperature region, the long time dynamics derived

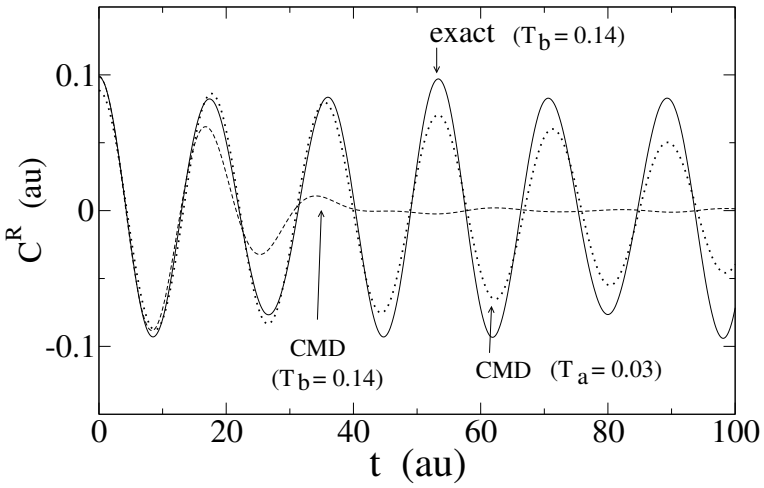

Figure 10. Comparison of the exact real part, $C^R(t)$, of the time correlation function of the position operator for the model potential V_q at temperature $T = 0.14$ a.u. with those results obtained from CMD approximations at temperatures $T = 0.14$ a.u. and $T = 0.03$ a.u.. The exact curve agrees better with the CMD result at low temperature.

by CMD has no physical meaning. However, the short time dynamics is predicted realistically.

6.3 Quantum Transmission Coefficients

The previous numerical results have shown that the RMD correction term, $\nu(X)$, for the mean force has little influence in the dynamics. In this Subsec. we check the influence of this term in the context of PI-QTST. The quantum correction factor to the classical rate constant is given within PI-QTST by[11,15]

$$\Gamma_{QTST} = \frac{e^{-\beta \Delta V_{ecp}}}{e^{-\beta \Delta V}} \tag{124}$$

where ΔV is the classical potential energy barrier, while ΔV_{ecp} is the corresponding barrier for V_{ecp}. This factor measures the enhancement of the quantum rate with respect to the classical one. If the coordinates X_i and X_b label the reactant and barrier positions, the quantity ΔV_{ecp} can be calculated as an integral of mean force

$$\Delta V_{ecp} = -\int_{X_i}^{X_b} f_m(X) dX \ . \tag{125}$$

If one includes the RMD correction term [see Eq. (99)], $\nu(X)$, in the integrand of the last equation, one gets a modified effective potential

$$\Delta V_{RMD} = \Delta V_{ecp} - \frac{1}{2\beta} \ln \frac{\delta x^2(X_b)}{\delta x^2(X_i)} \ . \tag{126}$$

By substituting ΔV_{RMD} by ΔV_{ecp} in the expression of Γ_{QTST}, we obtain the following quantum correction factor

$$\Gamma_{RMD} = \left[\frac{\delta x^2(X_b)}{\delta x^2(X_i)}\right]^{\frac{1}{2}} \Gamma_{QTST} \; . \tag{127}$$

The correction term, $\nu(X)$, leads to a simple dynamic factor in the PI-QTST expression for the rate constant. We have tested the capability of this expression to calculate, for a symmetric Eckart barrier, the transmission coefficient of an incident flux of protons (m=1836 a.u.), with initial velocities given by the classical Maxwell-Boltzmann distribution. The Eckart barrier is

$$V(x) = V_b \, \mathrm{sech}^2(x/a) \, . \tag{128}$$

The parameters defining the potential are the barrier height V_b = 0.2485 eV and the distance a = 0.3491 Å. These values have been chosen to correspond to the same physical situation as that studied in Refs.[15,35,36].

The quantum correction factor Γ evaluated exactly for the symmetric Eckart barrier is compared in Tab. 1 to the values of Γ_{QTST} and Γ_{RMD}. The column Γ_v was calculated using a dynamic preexponential factor derived by Gillan[11], and also by Cao and Voth.[35] The dynamic factor derived from the RMD equation provides a realistic result.

T (K)	Γ_{QTST}	Γ_v	Γ_{RMD}	Γ
10000	1.00	1.00	1.00	1.00
503.27	1.42	1.62	1.52	1.52
301.96	2.70	3.45	3.12	3.10
150.98	105.3	141.3	177.0	161.9
81.97	1.54×10^7	2.65×10^7	3.97×10^7	3.77×10^7
26.60	1.71×10^{37}	4.28×10^{37}	6.23×10^{37}	7.84×10^{37}

Table 1. Quantum correction factors for the symmetric Eckart barrier at several selected temperatures. Γ_{QTST} is the PI-QTST result. Γ_v was obtained by multiplying the value, Γ_{QTST}, by a previously derived dynamic factor (see text). Γ_{RMD} is calculated using the dynamic factor derived from the RMD approximation. Γ is the exact value.

7 A Review of CMD Applications

The numerical solution of the CMD equations is a classical molecular dynamics problem. However, the computation of the mean force, f_m, is a quantum problem that must be handled numerically by PI simulations and requires the use of efficient algorithms. Although a detailed account of these algorithms is outside the scope of the present chapter, we quote in the next Subsection some relevant literature. The subsequent Subsections present a review of CMD applications on noble gases, liquid p-H_2, water, anharmonic molecule vibrations, and vibrational energy relaxations.

7.1 Numerical Algorithms

The PI computation of the mean force, f_m, can be performed either by MC or MD simulations. However, most CMD applications use the adiabatic or "on the fly" PI MD method.[20,37,38] The setup of these simulations implies the transformation of the set of cartesian coordinates defining the "ring polymers" into a set of normal modes by a Fourier expansion. The centroid coordinate of each particle corresponds to the normal mode whose wave vector is zero. The centroid modes can be made the slowest moving modes in the MD simulation by assigning a sufficiently small mass to the non-centroid path modes. By virtue of the adiabatic principle, the slow degrees of freedom (the centroids) will move on the effective classical potential that is dynamically produced by the "on the fly" averaging of the non-centroid path modes. To ensure an ergodic exploration by PI MD it is also necessary to modify the dynamics of the normal modes by the attachment of a Nosé-Hoover chain thermostat to each normal mode.[39,40] A detailed theoretical account of the combination of ab initio Car-Parrinello molecular dynamics with CMD has been presented by Marx *et al.*,[41] while a similar implementation has been published by Pavese *et al.*.[42] The efficiency of CMD algorithms can be largely increased by the parallel implementation of the method.[43]

7.2 Noble Gases

The calculation of the diffusion constant of Ne at $T = 40K$ was one of the first test of the CMD approximation.[18] The interaction was described by a Lennard-Jones potential and the calculation of V_{ecp} was simplified by using the variational Feynman-Hibbs approximation.[1] The diffusion coefficient of the liquid was calculated as the time integral of the centroid velocity autocorrelation function. The CMD result is 7% lower than the value derived from a classical simulation.[18]

Miura *et al.*[44] have presented an interesting study of nonsuperfluid liquid ^{4}He at 4 K. The diffusion coefficient and the power spectra of the velocity autocorrelation function were derived by CMD simulations. This work presents also a calculation of the dynamic structure factor, $S_{coh}(k,\omega)$, of the liquid. This is an important quantity that is measured by neutron scattering experiments. In numerical simulations, $S_{coh}(k,\omega)$ can be derived from the relaxation function of the density fluctuations, that is defined as a Kubo transformed correlation function

$$R_{coh}(\mathbf{k},t) = \frac{1}{N}\int_0^\beta \frac{d\tau}{\beta}\langle\hat{\rho}_{\mathbf{k}}(-i\tau)\hat{\rho}_{-\mathbf{k}}(t)\rangle \ , \tag{129}$$

where the density operator, $\hat{\rho}_{\mathbf{k}}$, is the following sum over the position operators, $\hat{\mathbf{r}}_{\mathbf{i}}$, of the N system particles

$$\hat{\rho}_{\mathbf{k}} = \sum_{i=1}^{N} e^{i\mathbf{k}\hat{\mathbf{r}}_{\mathbf{i}}} \ . \tag{130}$$

In addition to the CMD approximation, Miura *et al.*[44] make the assumption that the Kubo transformed time correlation function, $R_{coh}(\mathbf{k},t)$, can be approximated by the correlation function associated to density fluctuations of the centroid positions

$$R_{coh}(\mathbf{k},t) \approx \frac{1}{N}\{\rho^{(c)}_{\mathbf{k}}(0)\rho^{(c)}_{-\mathbf{k}}(t)\} \ , \tag{131}$$

where $\rho_{\mathbf{k}}^{(c)}$ is the number density associated to the centroid positions, $\mathbf{R_i}$,

$$\rho_{\mathbf{k}}^{(c)} = \sum_{i=1}^{N} e^{i\mathbf{k}\mathbf{R_i}} \ . \tag{132}$$

The assumption given in Eq. (131) has no physical justification, because the density operator $\hat{\rho}_{\mathbf{k}}$ is not a linear function of the position operator [see Eqs. (67) and (68)]. This assumption may lead to unphysical results, e.g., the value of the correlation function, $R_{coh}(\mathbf{k}, 0)$ at $t = 0$, is a static quantity that is incorrectly reproduced using Eq. (131) (see Fig. 3 of the original work).[44] Interestingly, several results derived for ^{4}He using this assumption show a remarkable agreement with experiment. In particular, the simulated dynamic structure factor, $S_{coh}(k, \omega)$, shows a satisfactory agreement with the experimental spectrum for $0.2 < k < 2.2$ Å^{-1}.

7.3 Liquid $para$-$\mathbf{H_2}$

Liquid p-H_2 has been focused of a large number of CMD investigations. The diffusion coefficient of p-H_2 was determined by CMD at T=14 and 25 K, showing a good agreement to experimental data.[38] CMD simulations on liquid p-H_2 were also performed to check: (i) the quality of a pairwise approximation to the many-body function, V_{ecp};[45] (ii) the performance of a parallel CMD algorithm.[43]

The diffusive and vibrational properties of clusters Li(p-H_2)$_n$ (n=13, 55, and 180) and of a p-H_2 slab containing a lithium impurity has been investigated by CMD.[46,47] The dynamic simulations focused on the computation of centroid mean square displacements and the power spectra of velocity autocorrelation functions. The generated centroid trajectories were analyzed to characterize the diffusion of the lithium impurity and the melting properties of the p-H_2 clusters.

Kinugawa[48] has presented a study of the dynamic structure factor, $S(k, \omega)$, of liquid p-H_2. This simulation is the first calculation of $S(k, \omega)$ by a CMD approach supplemented by the assumption in Eq. (131). The calculated spectral profile indicates the existence of collective dynamics modes in this quantum liquid of Boltzmann particles. The predicted profiles were experimentally confirmed by two different neutron scattering experiments performed *after* the simulations.[49,50] The agreement between simulation data and experimental results is remarkable, specially because the approximation used to derive the simulation data has not sound theoretical justification.

7.4 Water and Proton Transport in Water

The influence of quantum effects in the dynamic properties of water at T=300 K has been studied by CMD using an empirical potential to describe the interatomic interactions.[51] Information on both collective and individual relaxation processes were derived from the study of several time correlation functions. The Debye dielectric relaxation time is the time constant associated to the exponential decay of the collective dipole moment correlation function. The rotational correlation time is associated to a single molecule time correlation function that depends on the molecule orientation with respect to a body-fixed reference frame. The correlation times derived by CMD are lower than the values obtained from a

classical simulation. This faster decay of the quantum correlation functions with respect to the classical ones, is also consistent with the larger value of the self-diffusion coefficient derived under inclusion of quantum effects. The simulation results for the time constants and the self-diffusion coefficient deviate significantly from the experimental values, probably due to deficiencies of the employed empirical potential. The wave numbers of the three intramolecular vibrational modes were derived from the power spectra of the velocity time autocorrelation function, showing a red shift of about 100 cm^{-1} with respect to the results of a classical simulation.[51]

Another CMD simulation has been presented using a different empirical potential for water.[52] In this simulation, the effective classical potential, V_{ecp} was approximated by a simple Feynman-Hibbs approach.[1] Unfortunately, the use of different empirical potentials precludes the comparison of CMD results derived with and without the use of the Feynman-Hibbs approximation.[52,51]

The proton transport in water has been studied by CMD using a two state[53] and a multistate empirical valence model (EVB).[54] Schmitt *et al.* undergo an analysis of the CMD trajectories in order to determine the rate constant for proton transport in water. This analysis is complicated because of the fluxional character of the excess proton, that can be associated to either the solvated Zundel ($H_5O_2^+$) and Eigen ($H_9O_4^+$) cations only as limiting ideal structures.[55] The rate constant was evaluated using a population autocorrelation function formalism, where selected many-body reaction coordinates were used to define different proton hopping pathways. The quantum rate was found to be two times faster compared to a classical treatment, and in good agreement to the experimental value.[54] The same simulation methodology was applied to study the kinetic H/D isotope effect in the proton transfer, resulting in an overestimation of this effect by about 25% with respect to the experimental value.[56]

7.5 Anharmonic Molecule Vibrations

CMD can be applied to the determination of vibrational frequencies, by means of the calculation of the power spectra derived from either the velocity or position autocorrelation functions of the atomic nuclei. Calculations of this type has been presented for small molecules, as H_2,[41], a linear chain of four water molecules,[42] and $Cl^-(H_2O)_n$ clusters.[57] While the position of the peaks in the power spectra are expected to be a realistic approximation of the vibrational frequencies, Marx. *et al.* pointed out that the width of the peaks in the power spectra are most likely an artifact inherent to the CMD approach.[41] This conclusion in in agreement with the model study presented in Sec. 6. At temperatures where the molecule is in its vibrational ground state, the width of the CMD power spectra, is due to the anharmonicity of the effective classical. We have already shown that these anharmonic regions in the V_{ecp} lead to unphysical dynamic results. Therefore, one should be aware of the limitations of the CMD procedure to study temperature effects in the vibrational spectra. An alternative to the CMD method for the determination of vibrational frequencies has been presented recently.[33] This method is based on the diagonalization of the covariance tensor of the position centroid fluctuations, as determined by equilibrium (nondynamic) simulations. The capability of this approximation has been tested in the study of the tunneling frequency of a particle in a double-well potential, the vibrational frequencies of molecules (H_2, C_2H_4 and HOCl), and the phonon frequencies of diamond.[33,58]

7.6 Vibrational Energy Relaxation

Two different strategies have been employed for the CMD simulation of vibrational energy relaxation. The first, and more direct approach, is to run a CMD simulation with a prepared initial condition, so that the vibrational degree of freedom to be relaxed is initially excited through an internal potential energy boost. The energy dissipation is then monitored along the CMD run. This approach has been applied to study the relaxation rate of a CN^- ion in water.[59] The second approach is based on the use of a golden rule formula for the thermal rate, which requires the determination of the time autocorrelation function of the bath quantum force operator. This approach has not been yet applied to real systems, the main efforts aimed at the test of different approximations to simplify the calculation of the force autocorrelation function.[60–62]

8 Open Problems

In some sense, the CMD approach is not an approximation, but a set of different approximations under a common name. Thus, at temperature $T \to 0$, CMD is a wave packet dynamics, while at $T \to \infty$, CMD is Newton dynamics. The dynamic character of the CMD equations changes with temperature because the effective classical potential changes with temperature. The curves shown in Fig. 10 provide a striking example of this change: CMD results are shown at two temperatures, $T_a < T_b$. CMD at temperature T_a is a reasonable approximation to the exact result at T_b, while CMD at T_b deviates more from the exact result at T_b. The physical conditions where the effective classical potential provides meaningful dynamic information in vibrational and diffusive problems need to be further characterized.

A second important problem is that CMD is an approximation for the simulation of time correlation functions of a product of an arbitrary operator with a position or momentum operator. Several recipes for the calculation of time correlation functions of nonlinear operators has been the subject of theoretical investigations.[19,63] However, from a practical point of view it is not clear which is the most convenient way to deal with nonlinear operators. In particular, it is important to clarify the calculation of the dynamic structure factor, $S(k, \omega)$, of liquids by CMD simulations.

Another interesting problem is the extension of CMD to the study of boson and fermions.[64,65,69] Several groups are working on this extension following different approaches. Two different methods define so-called permutation potentials in order to mimic the effect of the indistinguishability of the particles.[66–68] Thus, the Bose/Fermi system is mapped onto a pseudo-Boltzmann system where CMD is used to approximate Kubo transformed time correlation functions. The role of the permutation potential in the dynamic calculation requires careful study that leads to unexpected results. In this line, Kinugawa has shown that the time correlation function for position operators can be derived from the CMD trajectories in the pseudo-Boltzmann system, but not such relation appears for the momentum operator.[67] The latest formulation of CMD for Bose/Fermi systems shows the convenience of using an operator formalism without any reference to path integral techniques.[70]

9 Conclusions

The rigorous formulation of CMD turns out to be a cumbersome task. It is much easier to explain how to perform a CMD simulation (see the Introduction) than to explain, in quantum mechanical terms, the physical meaning of this dynamic approach (see Sections 4 and 5). Even more difficult is to specify the cases where CMD leads to correct results for describing real time quantum dynamics of many-body systems at finite temperature. This latter point is surely an important issue for future research.

In this chapter we have focused on the Schrödinger formulation of CMD. Although for historical reasons the original CMD formulation was based on the path integral approach, it has become clear that the most sensible way to formulate this approximation is using an operator formalism in the Schrödinger formulation. However, one can not avoid the path integral formulation, because the only feasible way to perform many-body CMD simulations is via path integrals.

Proceeding along this line we have found a slightly different approach (RMD), that differs from CMD by the presence of two correction terms (one for the mass and the other for the force) that modify the CMD equations. Test calculations performed on simple one dimensional models show that these correction terms improve the dynamic description in some special cases (description of quantum tunneling in the zero temperature limit and calculation of quantum transmission rates), but their influence is negligible in most cases. For this reason, we do not believe that the RMD equations represent a practical alternative to improve CMD.

One conclusion of our work is that it is not realistic to expect that a modification of the CMD equations (as RMD does) will lead to a significant improvement of the dynamic description. The reason is that the main source of error in CMD is not the dynamic equations used to propagate the centroid coordinates. The main limitation of CMD is a consequence of being *a constrained dynamic approximation*, i.e., the dynamic states accessible along the time evolution are severely limited. These states corresponds to fixed centroid path integrals and we do not see any feasible way to avoid the limitation of using fixed centroid path integrals in the constrained dynamics.

Acknowledgments

This work was supported by CICYT (Spain) under contract BFM2000-1318, and by DGESIC through Project No. 1FD97-1358.

References

1. R.P. Feynman and A.R. Hibbs, *Quantum Mechanics and Path Integrals* (McGraw-Hill, New York, 1965).
2. D.M. Ceperley, *Path integral theory and methods for ^4He*, Rev. Mod. Phys. **67**, 279 (1995).
3. C. Chakravarty, *Path integral simulations of atomic and molecular systems*, Inter. Rev. Phys. Chem. **16**, 421 (1997).

4. M.J. Gillan, *The path-integral simulation of quantum systems*, in *Computer Modelling of Fluids, Polymers, and Solids*, edited by C.R.A. Catlow, S.C. Parker, and M.P. Allen (Kluwer, Dordrecht, 1990).
5. B.J. Berne and D. Thirumalai, *On the simulation of quantum systems: path integral methods*, Ann. Rev. Phys. Chem. **37**, 401 (1987).
6. R. Giachetti and V. Tognetti, *Quantum corrections to the thermodynamics of nonlinear systems*, Phys. Rev. B**33**, 7647 (1986).
7. R.P. Feynman and H. Kleinert, *Effective classical partition functions*, Phys. Rev. A**34**, 5080 (1986).
8. H. Kleinert, *Path Integrals* (World Scientific, Singapore, 1995).
9. A. Cuccoli, R. Giachetti, V. Tognetti, R. Vaia, and P. Verrucchi, *The effective potential and effective Hamiltonian in quantum statistical mechanics*, J. Phys.: Condens. Matter **7**, 7891 (1995).
10. M. J. Gillan, *Quantum simulation of hydrogen in metals* Phys. Rev. Lett. **58**, 563 (1987).
11. M. J. Gillan, *Quantum-classical crossover of the transition rate in the damped double well*, J. Phys. C: Solid State Phys. **20**, 3621 (1987).
12. M. J. Gillan, *The quantum simulation of hydrogen in metals*, Phil. Mag. A **58**, 257 (1988).
13. G.A. Voth, *Path-integral centroid methods in quantum statistical mechanics and dynamics*, in *Advances in Chemical Physics, Vol. XCIII*, edited by I. Prigogine and S.A. Rice (John Wiley & Sons, New York, 1996).
14. G.A. Voth, *Feynman path integral formulation of quantum mechanical transition-state theory*, J. Phys. Chem. **97**, 8365 (1993).
15. G.A. Voth, D. Chandler, and W.H. Miller, *Rigorous formulation of quantum transition state theory and its dynamical corrections*, J. Chem. Phys. **91**, 7749 (1989).
16. J. Cao and G.A. Voth, *A new perspective on quantum time correlation functions*, J. Chem. Phys. **99** , 10070 (1993).
17. J. Cao and G.A. Voth, *The formulation of quantum statistical mechanics based on the Feynman path centroid density. I. Equilibrium properties*, J. Chem. Phys. **100**, 5093 (1994).
18. J. Cao and G.A. Voth, *The formulation of quantum statistical mechanics based on the Feynman path centroid density. II. Dynamical properties*, J. Chem. Phys. **100**, 5106 (1994).
19. J. Cao and G.A. Voth, *The formulation of quantum statistical mechanics based on the Feynman path centroid density. III. Phase space formalism and analysis of centroid molecular dynamics*, J. Chem. Phys. **101**, 6157 (1994).
20. J. Cao and G.A. Voth, *The formulation of quantum statistical mechanics based on the Feynman path centroid density. IV. Algorithms for centroid molecular dynamics*, J. Chem. Phys. **101**, 6168 (1994).
21. S. Jang and G.A. Voth, *Path integral centroid variables and the formulation of their exact real time dynamics*, J. Chem. Phys. **111**, 2357 (1999).
22. S. Jang and G.A. Voth, *A derivation of centroid molecular dynamics and other approximate time evolution methods for path integral centroid variables*, J. Chem. Phys. **111**, 2371 (1999).
23. G.A. Voth, *Feynman path centroid methods for condensed phase quantum dynamics*,

in *Classical and Quantum Dynamics in Condensed Phase Simulations*, edited by B.J. Berne, G. Ciccoti, and D.F. Coker (World Scientific, Singapore, 1998).
24. R. Ramírez and T. López-Ciudad, *Phase-space formulation of thermodynamic and dynamical properties of quantum particles*, Phys. Rev. Lett. **83**, 4456 (1999).
25. M.S. Swanson, *Path Integrals and Quantum Processes* (Academic Press, San Diego, 1992).
26. B. van der Pol and H. Bremmer, *Operational Calculus based on the two-sided Laplace Integral* (Chelsea, New York, 1995).
27. R.P. Feynman, *Statistical Mechanics* (Addison-Wesley, Redwood City, 1972).
28. T. López-Ciudad and R. Ramírez, *Spectral decomposition and Bloch equation of the operators represented by fixed-centroid path integrals*, J. Chem. Phys. **113**, 10849 (2000).
29. R. Kubo, M. Toda, and N. Hashitsume, *Statistical Physics II* (Springer-Verlag, Berlin, 1985).
30. R. Zwanzig, *Time-correlation functions and transport coefficients in statistical mechanics*, Ann. Rev. Phys. Chem. **16**, 67 (1969).
31. R. Ramírez, T. López-Ciudad, and J.C. Noya, *Feynman effective classical potential in the Schrödinger formulation*, Phys. Rev. Lett. **81**, 3303 (1998).
32. R. Ramírez and T. López-Ciudad, *The Schrödinger formulation of the Feynman path centroid density*, J. Chem. Phys. **111**, 3339 (1999).
33. R. Ramírez and T. López-Ciudad, *Low lying vibrational excitation energies from equilibrium path integral simulations*, J. Chem. Phys. **115**, 103 (2001).
34. G. Krilov and B.J. Berne, *Real time quantum correlation functions.I. Centroid molecular dynamics of anharmonic systems*, J. Chem. Phys. **111**, 9140 (1999).
35. J. Cao and G.A. Voth, *A unified framework for quantum activated rate processes. I. General theory*, J. Chem. Phys. **105**, 6856 (1996).
36. R. Ramírez, *Dynamics of quantum particles by path-integral centroid simulations: The symmetric Eckart barrier*, J. Chem. Phys. **107**, 3550 (1997).
37. G.J. Martyna, *Adiabatic path integral molecular dynamics methods. I. Theory*, J. Chem. Phys. **104**, 2018 (1996).
38. J. Cao and G.J. Martyna, *Adiabatic path integral molecular dynamics methods. II. Algorithms*, J. Chem. Phys. **104**, 2028 (1996).
39. G.J. Martyna, M.L. Klein, and M. Tuckerman, *Nosé-Hoover chains: The canonical ensemble via continuous dynamics*, J. Chem. Phys. **97**, 2635 (1992).
40. M.E. Tuckerman, D. Marx, M.L. Klein, and M. Parrinello, *Efficient and general algorithms for path integral Car-Parrinello molecular dynamics*, J. Chem. Phys. **104**, 5579 (1996).
41. D. Marx, M.E. Tuckerman, and G.J. Martyna, *Quantum Dynamics via adiabatic ab initio centroid molecular dynamics*, Computer Phys. Comm. **118**, 166 (1999).
42. M. Pavese, D.R. Berard, and G.A. Voth, *Ab initio centroid molecular dynamics: a fully quantum method for condensed-phase dynamics simulations*, Chem. Phys. Lett. **300**, 93 (1999).
43. A. Calhoun, M. Pavese, and G.A. Voth, *Hyper-parallel algorithms for centroid molecular dynamics: application to liquid para-hydrogen*, Chem. Phys. Lett. **262**, 415 (1996).
44. S. Miura, S. Okazaki, and K. Kinugawa, *A path integral centroid molecular dynamics*

study of nonsuperfluid liquid helium-4, J. Chem. Phys. **110**, 4523 (1999).
45. M. Pavese and G.A. Voth, *Pseudopotentials for centroid molecular dynamics. Application to self-diffusion in liquid para-hydrogen*, Chem. Phys. Lett. **249**, 231 (1996).
46. K. Kinugawa, P.B. Moore, and M.L. Klein, *Centroid path integral molecular dynamics simulation of lithium para-hydrogen clusters*, J. Chem. Phys. **106**, 1154 (1997).
47. K. Kinugawa, P.B. Moore, and M.L. Klein, *Centroid path integral molecular-dynamics studies of a para-hydrogen slab containing a lithium impurity*, J. Chem. Phys. **109**, 610 (1998).
48. K. Kinugawa, *Path integral centroid molecular dynamics study of the dynamic structure factors of liquid para-hydrogen*, Chem. Phys. Lett. **292**, 454 (1998).
49. F.J. Bermejo, K. Kinugawa, C. Cabrillo, S.M. Bennington, B.Fåk, M.T. Fernández-Díaz, P. Verkerk, J. Dawidowski, and R. Fernández-Perea, *Quantum effects on liquid dynamics as evidenced by the presence of well-defined collective excitations in liquid $para$-hydrogen*, Phys. Rev. Lett. **84**, 5359 (2000).
50. M. Zoppi, D. Colognesi, and M. Celli, *Microscopic dynamics of liquid hydrogen*, Europhys. Lett. **53**, 34 (2001).
51. J. Lobaugh and G. A. Voth, *A quantum model for water: Equilibrium and dynamical properties*, J. Chem. Phys. **106**, 2400 (1997).
52. B. Guillot and Y. Guissani, *Quantum effects in simulated water by the Feynman-Hibbs approach*, J. Chem. Phys. **108**, 10162 (1998).
53. J. Lobaugh and G. A. Voth, *The quantum dynamics of an excess proton in water*, J. Chem. Phys. **104**, 2056 (1996).
54. U.W. Schmitt and G.A. Voth, *The computer simulation of proton transport in water*, J. Chem. Phys. **111**, 9361 (1999).
55. D. Marx, M.E. Tuckerman, J. Hutter, and M. Parrinello, *The nature of hydrated excess proton in water*, Nature, **397**, 601 (1999).
56. U.W. Schmitt and G.A. Voth, *The isotope substitution effect on the hydrated proton*, Chem. Phys. Lett. **329**, 36 (2000).
57. G.K. Schenter, B. C. Garrett, and G.A. Voth, *The quantum vibrational structure of $Cl^-(H_2O)_n$ clusters*, J. Chem. Phys. **113**, 5171 (2000).
58. R. Ramírez, J. Schulte, and M.C. Böhm, *Ground state and excited state properties of ethylene isomers studied by a combined Feynman path integral-ab initio approach*, Mol. Phys. **99**, 1249 (2001).
59. S. Jang, Y. Pak, and G.A. Voth, *Quantum dynamical simulation of the energy relaxation rate of the CN^- ion in water*, J. Phys. Chem. A**103**, 10289 (1999).
60. J. Poulsen, S. Keiding, and P.J. Rossky, *Extracting rates of vibrational energy relaxation from centroid molecular dynamics*, Chem. Phys. Lett. **336**, 448 (2001).
61. J.A. Poulsen and P.J. Rossky, *An ansatz-based variational path integral centroid approach to vibrational energy relaxation in simple liquids*, J. Chem. Phys. **115**, 8014 (2001).
62. J.A. Poulsen and P.J. Rossky, *Path integral centroid molecular-dynamics evaluation of vibrational energy relaxation in condensed phase*, J. Chem. Phys. **115**, 8024 (2001).
63. D.R. Reichman, P.-N. Roy, S. Jang, and G.A. Voth, *A Feynman path centroid dynamics approach for the computation of time correlation functions involving nonlinear operators*, J. Chem. Phys. **113**, 919 (2000).
64. P.-N. Roy and G.A. Voth, *On the Feynman path centroid density for Bose-Einstein*

and Fermi-Dirac statistics, J. Chem. Phys. **110**, 3647 (1999).
65. P.-N. Roy, S. Jang, and G.A. Voth, *Feynman path centroid dynamics for Fermi-Dirac statistics*, J. Chem. Phys. **111**, 5303 (1999).
66. K. Kinugawa, H. Nagao, and K. Ohta, *Path integral centroid molecular dynamics method for Bose and Fermi statistics: formalism and simulation*, Chem. Phys. Lett. **307**, 187 (1999).
67. K. Kinugawa, H. Nagao, and K. Ohta, *A semiclassical approach to the dynamics on many-body Bose/Fermi systems by the path integral centroid molecular dynamics*, J. Chem. Phys. **114**, 1454 (2001).
68. S. Miura and S. Okazaki, *Path integral molecular dynamics method based on a pair density matrix approximation: An algorithm for distinguishable and identical particle systems*, J. Chem. Phys. **115**, 5353 (2001).
69. N.V. Blinov, P.-N. Roy and G.A. Voth, *Path integral formulation of centroid dynamics for systems obeying Bose-Einstein statistics*, J. Chem. Phys. **115**, 4484 (2001).
70. N.V. Blinov and P.-N. Roy *Operator formulation of centroid dynamics for Bose-Einstein and Fermi-Dirac statistics*, J. Chem. Phys. **115**, 7822 (2001).